UNIVERSIDADE ESTADUAL PAULISTA
"JÚLIO DE MESQUITA FILHO"
FACULDADE DE MEDICINA

David Rafael Abreu Reyes

INFLUÊNCIA DO EXERCÍCIO FÍSICO E DA N-ACETILCISTEÍNA NO REMODELAMENTO CARDÍACO E ESTRESSE OXIDATIVO DE RATOS COM SOBRECARGA PRESSÓRICA CRÔNICA

Tese apresentada à Faculdade de Medicina, Universidade Estadual Paulista "Júlio de Mesquita Filho", Câmpus de Botucatu, para obtenção do título de Doutor em Fisiopatologia em Clínica Médica.

Orientadora: Profª. Adj. Dra. Marina Politi Okoshi
Coorientador: Prof. Dr. Ricardo Luiz Damatto
Profa. Dra. Camila Moreno Rosa

Botucatu
(2017)

David Rafael Abreu Reyes

Influência do Exercício Físico e da N-Acetilcisteína no Remodelamento Cardíaco e Estresse Oxidativo de Ratos com Sobrecarga Pressórica Crônica

Tese apresentada à Faculdade de Medicina, Universidade Estadual Paulista "Júlio de Mesquita Filho", Câmpus de Botucatu, para obtenção do título de Doutor em Fisiopatologia em Clínica Médica.

Orientadora: Profª. Adj. *Marina P Okoshi*

Co-orientadores: Prof. Dr. *Ricardo Luiz Damatto*

Profa. Dra. *Camila Moreno Rosa*

Botucatu
2017

FICHA CATALOGRÁFICA ELABORADA PELA SEÇÃO TÉC. AQUIS. TRATAMENTO DA INFORM.
DIVISÃO TÉCNICA DE BIBLIOTECA E DOCUMENTAÇÃO - CÂMPUS DE BOTUCATU - UNESP

BIBLIOTECÁRIA RESPONSÁVEL: ROSEMEIRE APARECIDA VICENTE-CRB 8/5651

Reyes, David Rafael Abreu.
Influência do exercício físico e da N-Acetilcisteína no remodelamento cardíaco e estresse oxidativo de ratos com sobrecarga pressórica crônica / David Rafael Abreu Reyes. - Botucatu, 2017

Tese (doutorado) - Universidade Estadual Paulista "Júlio de Mesquita Filho", Faculdade de Medicina de Botucatu
Orientador: Adjunta Marina Politi Okoshi
Coorientador: Ricardo Luiz Damatto
Coorientador: Camila Moreno Rosa
Capes: 40101002

1. Remodelação ventricular. 2. Stress oxidativo. 3. Estenose da válvula aórtica. 4. Exercícios físicos.

Palavras-chave: Estenose aórtica; Estresse oxidativo; Exercício; N-Acetilcisteína; Remodelação cardíaca.

Agradecimentos

À Deus, por abençoar minha vida com pessoas maravilhosas e por todas as conquistas alcançadas.

Aos meus pais, David e Marisa, esposa e filho, meus exemplos, por serem inspiração em minha vida, sempre me apoiarem em todas as decisões, mesmo que elas pudessem nos distanciar, por não medirem esforços para me verem feliz. A todos da minha família, pelos conselhos e ensinamentos, pelo afeto, alegria e apoio.

À Profa. Adjunto Marina pela confiança, apoio incondicional, exemplo de pesquisadora e professional excelente.

Ao Prof. Adjunto Dr. Katashi Okoshi, pela realização da avaliação ecocardiográfica de todos os animais.

À Profa. Dra. Ana Angélica Henrique Fernandes, pela análise das enzimas antioxidantes, realizada no Laboratório de Pesquisa do Departamento de Química e Bioquímica do Instituto de Biociências de Botucatu, UNESP.

Ao amigo Dijon Campos, pela cirurgia para indução de estenose aórtica nos animais e pela amizade.

A todos os colegas da Unipex, Mariana, Camila Rosa, Camila Garcia, Felipe, Marcelo, Luana, Ricardo, Eder, Tierres, Adriana, Paula Grippa, Diego, Danilo, De Lalla, Igor, Lucas, Regina, Renata, Rogério, Sueli, Cristiane, Mara, José Carlos Georgete, Marta, Paulinho, Vítor, Guiomar, Leandro, Marcia, Silvia, Cristiane, Sara, pela colaboração para realização deste trabalho,

A todos meus amigos cubanos por seu apoio nos momentos difíceis, a Cris, Artur, Suelen,

Aos funcionários do Departamento de Clínica Médica, Ana Maria Mengue, Laura Andrade Câmara, Mário Augusto, Bruno José Faiolli, Elisângela Aparecida da Silva, pela dedicação e simpatia com que sempre me ajudaram,

Aos Funcionários da Seção de Pós Graduação, Vania Soler, Diego, Janette, Sergio, pela disponibilidade e eficiência para resolver problemas.

À apoio de Fapesp, CNPq e AUIP/PAEDEx.

A todas as pessoas que fizeram parte da minha vida, contribuindo para minha formação profissional e pessoal.

Muito obrigado!

Summary

Introdução

Introdução

A insuficiência cardíaca (IC) é uma das principais causas de morbidade e mortalidade no mundo. A IC pode ser definida como síndrome clínica complexa que resulta de anormalidades cardíacas estruturais e/ou funcionais, adquiridas ou hereditárias, que comprometem a capacidade de enchimento e ejeção ventricular [1].

Aproximadamente 5,1 milhões de americanos têm IC, e a cada ano 550.000 novos casos são diagnosticados nos Estados Unidos. As causas mais comuns são a hipertensão arterial sistêmica, doença arterial coronariana, miocardiopatias e doença valvar [2]. Apesar do avanço considerável em seu tratamento, principalmente nas últimas décadas, a mortalidade por IC continua elevada. Em pacientes em classes funcionais II e III, recebendo tratamento otimizado, inclusive ressincronizador e desfibrilador implantável, a mortalidade por IC ainda é de aproximadamente 30 % em seis anos [3]. O mau prognóstico da doença mostra que mecanismos fisiopatológicos importantes ainda permanecem inalterados pelas modalidades terapêuticas atuais.

Independentemente da etiologia da IC, após a agressão cardíaca inicial, ocorrem alterações gênicas, moleculares, celulares, intersticiais e funcionais, que manifestam-se, clinicamente, como modificações no tamanho, forma e função do coração. Este processo é denominado remodelação cardíaca [4].

Atualmente, há substancial evidência que aumento do estresse oxidativo tenha papel importante na fisiopatologia da remodelação cardíaca e no desenvolvimento da IC [5]. O estresse oxidativo ocorre quando a geração de espécies reativas de oxigênio (EROs) supera a capacidade dos sistemas de defesa antioxidante. No miocárdio, o sistema de enzimas antioxidantes, composto pelas enzimas superóxido dismutase (SOD), glutationa peroxidase (GPX) e catalase (Cat), protege as células das ações das EROs. Na IC, observa-se aumento do estresse oxidativo tanto em nível sistêmico, como no miocárdio. Potencialmente importantes fontes de EROs na IC incluem a cadeia mitocondrial de transferência de elétrons, a xantina oxidase (XO), óxido nítrico sintase endotelial (eNOS), e NADPH oxidases [6].

No miocárdio insuficiente, a produção de EROs é aumentada na mitocôndria. Aumento crônico na produção de EROs mitocondrial gera declínio funcional da atividade mitocondrial, geração de mais EROs, e lesão celular. As EROs prejudicam diretamente a função contrátil, modificando a atividade de proteínas envolvidas no acoplamento excitação-contração. Além disso, as EROs ativam fatores de transcrição e vias intracelulares envolvidas na indução de apoptose. Adicionalmente, as EROs estimulam a proliferação de fibroblastos cardíacos e ativam metaloproteinases da matriz. Os eventos celulares acima descritos estão envolvidos na disfunção do miócito e no desenvolvimento e progressão da remodelação do miocárdio e da matriz extracelular.

Uma importante fonte produtora de estresse oxidativo no coração é a família da nicotinamida adenina dinucleotídeo fosfato (NADPH)-oxidase. Ela foi inicialmente descoberta em fagócitos, com a caracterização da isoforma NOX2, também referida como gp91phox. Mais recentemente, seis outros membros da família codificados por genes distintos foram identificados: NOX1, NOX3, NOX4, NOX5, dupla oxidase DUOX1 e DUOX2. As isoformas predominantemente expressas nos cardiomiócitos são a NOX2 e NOX4 [5] [6] . Estas isoformas diferem entre si quanto ao modo de ativação, à interação com a pequena proteína transmembrana p22phox e à necessidade adicional de fatores de maturação e ativação. A NOX2 forma um complexo com a p22phox, cuja ativação depende da ligação com as subunidades regulatórias citosólicas, p47phox e p67phox. Diferentemente das outras isoformas, a NOX4 é constitutivamente ativa e independente de proteínas citosólicas regulatórias ou ativadoras. A função das enzimas NADPH oxidase é catalisar a transferência de um elétron da NADPH para o oxigênio molecular, gerando EROs [7].

Em condições fisiológicas, a NADPH oxidase é quiescente. Entretanto, quando se torna ativada durante a contração muscular ou por estímulos infecciosos e pró-inflamatórios, a NADPH oxidase pode gerar grandes quantidades do ânion radical superóxido, que pode ser convertido em peróxido de hidrogênio (H_2O_2) pela enzima antioxidante superóxido dismutase [8]. A atividade da NADPH-oxidase pode ser exacerbada por vários estímulos geralmente presentes durante a IC como, por exemplo, estiramento mecânico do miócito, angiotensina II e

endotelina-1 [6] [8]. Estudos experimentais mostraram que a NOX4, localizada principalmente na mitocôndria de miócitos cardíacos, é responsável pela maior produção de EROs em situação de sobrecarga de pressão e envelhecimento [6] [8].

Aumento da atividade e da expressão da NADPH oxidase foi observado na hipertrofia ventricular esquerda (HVE) por sobrecarga de pressão e no infarto do miocárdio. Aumento do estresse oxidativo tem efeitos diretos sobre as estruturas e função cardíaca. O estresse oxidativo estimula a hipertrofia miocitária e a remodelação da matriz extracelular, e induz disfunção celular.

Quanto às vias de sinalização pelas quais o estresse oxidativo leva a alterações miocárdicas, há evidências que as vias das proteínas quinases ativadas por mitógeno (MAPKs) possam estar envolvidas [9]. As proteínas da via das MAPKs como a ERK1/2, JNK e p38 MAPK estão envolvidas no desenvolvimento de hipertrofia miocárdica e de IC [10]. As EROs podem, também, ativar as metaloproteases (MMP), uma família de enzimas proteolíticas, e induzir alterações da matriz extracelular [6].

O exercício físico tem sido considerado importante estratégia terapêutica não farmacológica na prevenção e reabilitação de muitas doenças cardiovasculares incluindo a IC crônica [11]. De acordo com a III Diretriz Brasileira de Insuficiência Cardíaca, exercícios físicos devem ser prescritos para pacientes com IC estável que sejam capazes de participar de programa de treinamento físico [12].

Os efeitos benéficos do treinamento físico no sistema cardiovascular estão associados a redução de ativação neuro-humoral e inflamatória sistêmica e melhora da função vascular. O exercício físico pode afetar positivamente o consumo máximo de oxigênio, a capacidade física, e a função cardíaca e autonômica do sistema nervoso, muscular esquelética e vascular periférica [11]. Embora sejam evidentes os benefícios do exercício, ainda não estão completamente identificados os mecanismos moleculares pelos quais o treinamento físico melhora a função ventricular durante a IC.

Entre os efeitos benéficos do exercício físico, destaca-se sua ação antioxidante. O exercício aumenta a expressão de enzimas antioxidantes e reduz a expressão de enzimas pró-oxidantes. O aumento na atividade de enzimas antioxidantes pode ser observado em vários tecidos, após treinamento aeróbio ou

anaeróbio [13] [14]. Os radicais livres produzidos durante a contração muscular atuam como moléculas de sinalização, estimulando a expressão gênica e aumentando a atividade de enzimas antioxidantes. Adicionalmente, modulam vias de proteção ao estresse oxidativo promovendo, por exemplo, aumento de enzimas reparadoras do DNA nos miocárdio [15] [16] [17] [18] .

Estudos experimentais mostraram que o treinamento físico aumenta a capacidade antioxidante do miocárdio e a expressão de proteínas relacionadas ao trânsito de cálcio tanto em animais saudáveis como naqueles com IC. Em vários estudos, foi observada a contribuição do treinamento físico para a melhora da expressão de marcadores da biogênese mitocondrial e do metabolismo oxidativo no miocárdio [19] [20] .

É importante salientar que a maioria dos estudos sobre os efeitos benéficos do exercício na IC foram realizados em modelos experimentais de isquemia miocárdica. Poucos trabalhos avaliaram os efeitos do exercício durante a sobrecarga pressórica crônica e sua transição para IC descompensada, condição de alta prevalência devida à elevada frequência de hipertensão arterial sistêmica e cardiopatia hipertensiva na população geral, e de estenose aórtica em idosos.

Apesar da importância do estresse oxidativo na indução de dano miocárdico, a terapia antioxidante ainda é assunto controverso no tratamento da IC [21] [22]. (A glutationa (L-γ glutamil-cisteinil-glicina) é um tripeptídeo endógeno que apresenta papel central na defesa celular contra o estresse oxidativo [23] A glutationa é sintetizada e mantida em elevadas concentrações nas células em geral [24] Na IC, ocorre alteração do estado redox da glutationa e sua concentração é reduzida no miocárdio [25] [26].

A N-acetilcisteína (NAC) é uma molécula com propriedades antioxidantes, que possui um grupo sulfidrila que age como fonte de cisteína para a síntese de glutationa. A administração de NAC resultou em restauração da concentração total de glutationa miocárdica e redução de marcadores do estresse oxidativo, como hidroperóxido de lipídeo e peróxido de hidrogênio, em ratos infartados [23] [25] [27].

Adicionalmente, a NAC atenuou hipertrofia cardíaca e miocitária, fibrose intersticial, disfunção ventricular, e propensão a arritmias em diferentes modelos de injúria cardíaca [26] [28] [29] [30].

Entretanto, os efeitos da NAC durante a transição de hipertrofia ventricular compensada para a IC clínica não foram avaliados.

Estenose aórtica ascendente em ratos jovens tem sido considerada bom modelo para estudo experimental da hipertrofia cardíaca e IC [31] [32] [33] [34]. Neste modelo, um clip de prata não obstrutivo é colocado ao redor da aorta ascendente. À medida que os animais crescem, passam a manifestar a estenose aórtica e a desenvolver hipertrofia ventricular esquerda concêntrica e disfunção diastólica. Mais tardiamente, ocorrem redução do desempenho ventricular sistólico e IC[32] [33].

Objetivo

Avaliar, isoladamente, a influência do exercício físico aeróbio e da administração de N-acetilcisteína sobre a função ventricular, o estresse oxidativo miocárdico e as vias de sinalização das MAPK em ratos com estenose aórtica durante a transição de sobrecarga pressórica crônica para insuficiência cardíaca clínica.

A seguir, apresentaremos os dois manuscritos que foram derivados deste estudo.

Referências

1. Greenberg B, Kahn A: Braunwald´s Heart Disease A textbook of cardiovascular medicine; in Bonow R, Mann D, Zipes D, Libby (eds): Braunwald´s Heart Disease A textbook of cardiovascular medicine, 9th ed. Philadelphia, Elsevier Saunders, 2012, pp 505-516.
2. Mozaffarian D, Benjamin EJ, Go AS, Arnett DK, Blaha MJ, Cushman M, et al.: Heart Disease and Stroke Statistics—2016 Update. Circulation 2016;133:e38-e360.
3. Khidir MJH, Delgado V, Ajmone Marsan N, Schalij MJ, Bax JJ: QRS duration versus morphology and survival after cardiac resynchronization therapy. ESC Hear Fail 2017;4:23-30.
4. Cohn JN, Ferrari R, Sharpe N: Cardiac remodeling--concepts and clinical implications: a consensus paper from an international forum on cardiac remodeling. Behalf of an International Forum on Cardiac Remodeling. J Am Coll Cardiol 2000;35:569-82.
5. Theccanat T, Philip JL, Razzaque AM, Ludmer N, Li J, Xu X, et al.: Regulation of cellular oxidative stress and apoptosis by G protein-coupled receptor kinase-2; The role of NADPH oxidase 4. Cell Signal 2016;28:190-203.
6. Matsushima S, Kuroda J, Zhai P, Liu T, Ikeda S, Nagarajan N, et al.: Tyrosine kinase FYN negatively regulates NOX4 in cardiac remodeling. J Clin Invest 2016;126:3403-16.
7. Sirker A, Murdoch CE, Protti A, Sawyer GJ, Santos CXC, Martin D, et al.: Cell-specific effects of Nox2 on the acute and chronic response to myocardial infarction. J Mol Cell Cardiol 2016;98:11-7.
8. Sag CM, Santos CXC, Shah AM: Redox regulation of cardiac hypertrophy. J Mol Cell Cardiol 2014;73:103-11.

9. Byun M-S, Jeon K-I, Choi J-W, Shim J-Y, Jue D-M, Lee S-S, et al.: Dual effect of oxidative stress on NF-kappakB activation in HeLa cells. Exp Mol Med 2002;34:332-9.

10. Okoshi MP, Yan X, Okoshi K, Nakayama M, Schuldt AJT, O'Connell TD, et al.: Aldosterone directly stimulates cardiac myocyte hypertrophy. J Card Fail 2004;10:511-8.

11. Alves AJ, Viana JL, Cavalcante SL, Oliveira NL, Duarte JA, Mota J, et al.: Physical activity in primary and secondary prevention of cardiovascular disease: Overview updated. World J Cardiol 2016;8:575-583.

12. Bocchi EA, Marcondes-Braga FG, Bacal F, Ferraz AS, Albuquerque D, Rodrigues D de A, et al.: [Updating of the Brazilian guideline for chronic heart failure - 2012]. Arq Bras Cardiol 2012;98:1-33.

13. Margaritelis N V, Theodorou AA, Paschalis V, Veskoukis AS, Dipla K, Zafeiridis A, et al.: Experimental verification of regression to the mean in redox biology: differential responses to exercise. Free Radic Res 2016;50:1237-1244.

14. Staiculescu MC, Foote C, Meininger GA, Martinez-Lemus LA: The role of reactive oxygen species in microvascular remodeling. Int J Mol Sci 2014;15:23792-835.

15. Kozakowska M, Pietraszek-Gremplewicz K, Jozkowicz A, Dulak J: The role of oxidative stress in skeletal muscle injury and regeneration: focus on antioxidant enzymes. J Muscle Res Cell Motil 2015;36:377-93.

16. Brown DI, Griendling KK: Regulation of signal transduction by reactive oxygen species in the cardiovascular system. Circ Res 2015;116:531-49.

17. Ennezat P V, Malendowicz SL, Testa M, Colombo PC, Cohen-Solal A, Evans T, et al.: Physical training in patients with chronic heart failure enhances the expression of genes encoding antioxidative enzymes. J Am Coll Cardiol 2001;38:194-8.

18. Gomes MJ, Martinez PF, Pagan LU, Damatto RL, Cezar MDM, Lima ARR, et al.: Skeletal muscle aging: influence of oxidative stress and physical exercise. Oncotarget 2017;8:20428-20440.

19. Ping Z, Zhang L, Cui Y, Chang Y, Jiang C, Meng Z, et al.: The Protective Effects of Salidroside from Exhaustive Exercise-Induced Heart Injury by Enhancing the PGC-1 α -NRF1/NRF2 Pathway and Mitochondrial Respiratory Function in Rats. Oxid Med Cell Longev 2015;2015:876825.

20. Hambrecht R, Fiehn E, Weigl C, Gielen S, Hamann C, Kaiser R, et al.: Regular physical exercise corrects endothelial dysfunction and improves exercise capacity in patients with chronic heart failure. Circulation 1998;98:2709-15.

21. Münzel T, Gori T, Keaney JF, Maack C, Daiber A: Pathophysiological role of oxidative stress in systolic and diastolic heart failure and its therapeutic implications. Eur Heart J 2015;36:2555-64.

22. Altenhöfer S, Radermacher KA, Kleikers PWM, Wingler K, Schmidt HHHW: Evolution of NADPH Oxidase Inhibitors: Selectivity and Mechanisms for Target Engagement. Antioxid Redox Signal 2015;23:406-27.

23. Fratelli M, Goodwin LO, Ørom UA, Lombardi S, Tonelli R, Mengozzi M, et al.: Gene expression profiling reveals a signaling role of glutathione in redox regulation. Proc Natl Acad Sci U S A 2005;102:13998-4003.

24. Rushworth GF, Megson IL: Existing and potential therapeutic uses for N-acetylcysteine: the need for conversion to intracellular glutathione for antioxidant benefits. Pharmacol Ther 2014;141:150-9.

25. Adamy C, Mulder P, Khouzami L, Andrieu-abadie N, Defer N, Candiani G, et al.: Neutral sphingomyelinase inhibition participates to the benefits of N-acetylcysteine treatment in post-myocardial infarction failing heart rats. J Mol Cell Cardiol 2007;43:344-53.

26. Lombardi R, Rodriguez G, Chen SN, Ripplinger CM, Li W, Chen J, et al.: Resolution of established cardiac hypertrophy and fibrosis and prevention of systolic dysfunction in a transgenic rabbit model of human cardiomyopathy through thiol-sensitive mechanisms. Circulation 2009;119:1398-407.

27. Bourraindeloup M, Adamy C, Candiani G, Cailleret M, Bourin M-C, Badoual T, et al.: N-acetylcysteine treatment normalizes serum tumor necrosis factor-alpha

level and hinders the progression of cardiac injury in hypertensive rats. Circulation 2004;110:2003-9.

28. Giam B, Chu P-Y, Kuruppu S, Smith AI, Horlock D, Kiriazis H, et al.: N-acetylcysteine attenuates the development of cardiac fibrosis and remodeling in a mouse model of heart failure. Physiol Rep 2016;4:e12757.

29. Wilder T, Ryba DM, Wieczorek DF, Wolska BM, Solaro RJ: N-acetylcysteine reverses diastolic dysfunction and hypertrophy in familial hypertrophic cardiomyopathy. Am J Physiol Heart Circ Physiol 2015;309:H1720-30.

30. Foltz WU, Wagner M, Rudakova E, Volk T: N-acetylcysteine prevents electrical remodeling and attenuates cellular hypertrophy in epicardial myocytes of rats with ascending aortic stenosis. Basic Res Cardiol 2012;107:290.

31. Weinberg EO, Lee MA, Weigner M, Lindpaintner K, Bishop SP, Benedict CR, et al.: Angiotensin AT1 receptor inhibition. Effects on hypertrophic remodeling and ACE expression in rats with pressure-overload hypertrophy due to ascending aortic stenosis. Circulation 1997;95:1592-600.

32. Ribeiro HB, Okoshi K, Cicogna AC, Bregagnollo EA, Rodrigues MAM, Padovani CR, et al.: Follow-up study of morphology and cardiac function in rats undergoing induction of supravalvular aortic stenosis. Arq Bras Cardiol 2003;81:569-75, 562-8.

33. Moreira VO, de Castro AVB, Yaegaschi MY, Cicogna AC, Okoshi MP, Pereira CA, et al.: [Echocardiographic criteria for the definition of ventricular dysfunction severity in aortic banded rats]. Arq Bras Cardiol 2006;86:432-8.

34. Moreira VO, Pereira CA, Silva MO, Felisbino SL, Cicogna AC, Okoshi K, et al.: Growth hormone attenuates myocardial fibrosis in rats with chronic pressure overload-induced left ventricular hypertrophy. Clin Exp Pharmacol Physiol 2009;36:325-30.

N-ACETYLCYSTEINE INFLUENCE ON OXIDATIVE STRESS AND CARDIAC REMODELING IN RATS DURING TRANSITION FROM COMPENSATED LEFT VENTRICULAR HYPERTROPHY TO HEART FAILURE

David RA Reyes[1], Mariana J Gomes[1], Camila M Rosa[1], Luana U Pagan[1], Felipe C Damatto[1], Ricardo L Damatto[1], Igor Depra[1], Dijon HS Campos[1], Ana AH Fernandez[2], Paula F Martinez[3], Katashi Okoshi[1], Marina P Okoshi[1]

[1] Department of Internal Medicine, Botucatu Medical School, Sao Paulo State University, UNESP, Botucatu, SP, Brazil

[2] Botucatu Institute of Biosciences, Sao Paulo State University, UNESP, Botucatu, SP, Brazil

[3] Federal University of Mato Grosso do Sul, Campo Grande, MS, Brasil

Correspondence author: Marina P Okoshi

Address: Faculdade de Medicina de Botucatu, Departamento de Clinica Medica. Rubiao Junior, S/N CEP 18.618-687 Botucatu, SP, Brazil

e-mail: mpoliti@fmb.unesp.br

Abstract

Objective. To evaluate the effects of *N*-acetylcysteine (NAC) on cardiac remodeling in rats during transition from compensated left ventricular (LV) hypertrophy to heart failure. **Methods and Results.** Four months after inducing aortic stenosis (AS), Wistar rats were assigned into three groups: Sham, AS, and AS treated with NAC (AS-NAC for eight weeks). NAC restored myocardial total glutathione (Sham 20.8±3.00; AS 12.6±2.92; AS-NAC 17.6±2.45 nmol/g tissue; $p<0.05$ AS vs Sham and AS-NAC). Malondialdehyde serum concentration was lower in AS-NAC and myocardial lipid hydroperoxide was higher in AS (Sham 199±48.1; AS 301±36.0; AS-NAC 181±41.3 nmol/g tissue). Glutathione peroxidase activity was lower in AS than Sham. Echocardiogram showed LV concentric hypertrophy and dysfunction before and after treatment. Tissue Doppler imaging (TDI) of mitral annulus systolic velocity and isovolumetric relaxation time were lower in AS than Sham; in AS-NAC these parameters were between those in Sham and AS and did not differ from either group. NAC reduced p-ERK and p-JNK protein expression, attenuated myocyte hypertrophy and myocardial fibrosis, and decreased lung congestion frequency. **Conclusion.** *N*-acetylcysteine restores myocardial total glutathione, reduces oxidative stress, improves MAPK signaling, and attenuates myocyte hypertrophy, myocardial fibrosis, and LV dysfunction in aortic stenosis rats.

Introduction

The transition from compensated left ventricular (LV) hypertrophy to heart failure is a critical event in patients with long-term pressure overload conditions such as systemic arterial hypertension and aortic stenosis [1]. Although several mechanisms may be involved in the development of heart failure, its pathophysiology is not completely understood [2-4].

Oxidative stress is often observed and considered to play an important role on pathological cardiac remodeling and the transition to cardiac failure [5, 6]. Despite the importance of oxidative stress in inducing myocardial damage, antioxidant therapy is still a matter of controversy in heart failure treatment [7, 8]. Glutathione (L-γ glutamyl-cysteinyl-glycine) is an endogenous tripeptide that plays a central role in cellular defense against oxidative stress [9]. It is synthesized and maintained at high concentrations in cells [10]. In heart failure, glutathione redox status changes and its total concentration decreases in myocardium [11, 12]. *N*-acetylcysteine (NAC) is a molecule with antioxidant properties; it possesses a sulfhydryl group which acts as a source of cysteine to glutathione synthesis. NAC administration has been shown to restore total glutathione levels and reduce oxidative stress in infarcted rat hearts [11]. Furthermore, NAC attenuates cardiac and myocyte hypertrophy, interstitial fibrosis, LV dysfunction, and arrhythmogenic propensity in different experimental cardiac injury models [12-15]. However, the effects of NAC during the transition from compensated LV hypertrophy to clinical heart failure have not been established.

Ascending aortic stenosis in rats is a useful model to study chronic pressure overload-induced cardiac remodeling. In this model, three-four week-old rats are subjected to a clip being placed around the ascending aorta. After clip placement, aorta diameter is preserved; as rats grow, stenosis and LV hypertrophy progressively develop. In this model, ventricular dysfunction and clinical heart failure occur slowly, similarly to what is seen in human chronic pressure overload [16, 17]. In this study, we evaluated the effects of NAC administration on systemic and myocardial oxidative stress and cardiac remodeling in rats during transition from compensated LV hypertrophy to heart failure.

Materials and Methods

Experimental groups

Male Wistar rats weighing 90-100 g were purchased from the Central Animal House, Botucatu Medical School, Sao Paulo State University, UNESP, Brazil. All experiments and procedures were approved by the Animal Experimentation Ethics Committee of Botucatu Medical School, which follows the guidelines established by the Brazilian College for Animal Experimentation (protocol number 1071/2014).

Rats were anaesthetized with a mixture of ketamine hydrochloride (50 mg/kg, i.m.) and xylazine hydrochloride (10 mg/kg, i.m.) and aortic stenosis (AS) was induced by placing a 0.6 mm stainless-steel clip on the ascending aorta via a median thoracic incision according to a previously described method [16]. During surgery, the rats were manually ventilated using positive pressure and given 1 mL of warm saline solution intraperitoneally. Sham operated rats were used as controls. All animals were housed in a temperature controlled room at 23 °C and kept on a 12-hour light/dark cycle. Food and water were supplied *ad libitum*.

Four months after surgery, rats were subjected to transthoracic echocardiogram to evaluate the degree of cardiac injury, and assigned to three groups: control (Sham, n=16), AS (n=22), and AS treated with *N*-acetylcysteine (AS-NAC, n=15). *N*-acetylcysteine (Sigma, St. Louis, MO, USA) was added to chow at a dosage of 120 mg/kg/day for eight weeks. At the end of the experimental period, rats were subjected to transthoracic echocardiogram and euthanized the next day. During euthanasia, we determined the presence or absence of clinical and pathological heart failure features. The clinical finding suggestive of heart failure was tachypnea/labored respiration. Pathologic assessment of heart failure included pleuropericardial effusion, atrial thrombi, ascites, hepatic congestion, pulmonary congestion (lung weight/body weight ratio higher than 2 standard deviations above Sham group mean), and right ventricular hypertrophy (right ventricle weight/body weight ratio higher than 0.8 mg/g) [18, 19].

Echocardiography

Cardiac structures and left ventricular (LV) function were evaluated by transthoracic echocardiogram and tissue Doppler imaging (TDI) using a commercially available echocardiograph (General Electric Medical Systems, Vivid S6 model, Tirat Carmel, Israel) equipped with a 5-11.5 MHz multifrequency transducer as previously described [20-22]. After anesthesia with ketamine hydrochloride (50 mg/kg) and xylazine hydrochloride (1 mg/kg) intramuscularly, the rats were placed in left lateral decubitus. A two dimensional parasternal short-axis view of the LV was obtained at the level of the papillary muscles. M-mode tracings were obtained from short-axis views of the LV at or just below the tip of the mitral-valve leaflets and at the level of the aortic valve and left atrium. M-mode images of the LV were printed on a black-and-white thermal printer (Sony UP-890MD) at a sweep speed of 200 mm/s. All structures were manually measured by the same observer (KO). Values obtained were the mean of at least five cardiac cycles on M-mode tracings. The following structural variables were measured: left atrium diameter (LA), LV diastolic and systolic diameters (LVDD and LVSD, respectively), LV diastolic (D) and systolic (S) posterior wall thickness (PWT) and septal wall thickness (SWT), and aortic diameter. Left ventricular mass (LVM) was calculated using the formula $[(LVDD + DPWT + DSWT)^3 - LVDD^3] \times 1.04$. LV relative wall thickness (RWT) was calculated by the formula $2 \times DPWT/LVDD$. LV function was assessed by the following parameters: endocardial fractional shortening (EFS), midwall fractional shortening (MFS), ejection fraction (EF), posterior wall shortening velocity (PWSV), early and late diastolic mitral inflow velocities (E and A waves), E/A ratio, E-wave deceleration time (EDT), and isovolumetric relaxation time (IVRT). A joint assessment of diastolic and systolic LV function was performed using the myocardial performance index (Tei index). The study was complemented with evaluation by TDI of systolic (S'), early diastolic (E'), and late diastolic (A') velocity of the mitral annulus (arithmetic average of the lateral and septal walls) and E/E' ratio [23].

Collection of left ventricle and other tissues

One day after final echocardiogram, the rats were weighed and anesthetized with intraperitoneal sodium pentobarbital (50 mg/kg) and euthanized. After blood collection, hearts were removed by thoracotomy. Atria and ventricles were dissected, weighed separately, frozen in liquid nitrogen, and stored at −80 °C. Lung weight was used to assess the degree of pulmonary congestion [24].

Morphologic study

Frozen LV samples were transferred to a cryostat and cooled to -20°C. Serial transverse 8 μm thick sections were stained with hematoxylin and eosin. At least 50 cardiomyocyte diameters were measured from each LV as the shortest distance between borders drawn across the nucleus [25]. Other slides were stained with Sirius red F3BA and used to quantify interstitial collagen fraction [26]. On average, 20 microscopic fields were analyzed with a 40X lens. Perivascular collagen was excluded from this analysis. Measurements were taking using a microscope (Leica DM LS; Nussloch, Germany) attached to a computerized imaging analysis system (Media Cybernetics, Silver Spring, MD, USA).

Oxidative stress evaluation

Myocardial glutathione concentration

Reduced glutathione was determined using a kinetic method in media consisting of 100 mM phosphate buffer pH 7.4 containing 5 mM EDTA, 2 mM 5.5'-dithiobis-(2-nitrobenzoic) acid (DTNB), 0.2 mM NADPH2 and 2 U of glutathione reductase according to a previously describe method [27]. Total glutathione was measured in the presence of 0.1 M Tris-HCl buffer, pH 8.0 with 0.5 mM EDTA, 0.6 mM DTNB and 0.1 U glutathione reductase [27].

Antioxidant enzymes activity and lipid hydroperoxide concentration

Left ventricular samples (~200 mg) were homogenized in 5 mL of cold 0.1 M phosphate buffer, pH 7.0. Tissue homogenates were prepared in a motor-driven Teflon glass Potter-Elvehjem tissue homogenizer. The homogenate was centrifuged at 10,000 g, for 15 min at 4 °C, and the supernatant was assayed for total protein, lipid hydroperoxide [28], and glutathione peroxidase (GSH-Px, E.C.1.11.1.9), catalase (E.C.1.11.1.6.), and superoxide dismutase (SOD, E.C.1.15.1.1.) activities by spectrophotometry [29]. Enzyme activities were analyzed at 25 °C using a microplate reader (μQuant-MQX 200) with KCjunior software for computer system control (Bio-Tech Instruments, Winooski, Vermont, USA). Spectrophotometric determinations were performed in a Pharmacia Biotech spectrophotometer with temperature controlled cuvette chamber (UV/visible Ultrospec 5000 with Swift II applications software for computer system control, Cambridge, UK). All reagents were purchased from Sigma-Aldrich (St. Louis, MO, USA).

Malondialdehyde serum concentration

Systemic lipid peroxidation was assessed by measuring malondialdehyde (MDA) by high performance liquid chromatography (HPLC), as previously reported [30]. Briefly, 100 μL of serum were treated with 700 μL of 1% orthophosphoric acid and vortex-mixed for 10 s for protein precipitation. Then, 200 μL of thiobarbituric acid (TBA) were added. The mixture was heated to 100 ºC for 60 min and cooled to -20 ºC for 10 min. Then, 200 μL of this reaction were added to a solution containing 200 μL of NaOH:methanol (1:12). The tubes were centrifuged for 3 min at 13,000 g; 200 μL of the supernatant were taken for injection in the equipment. Analysis was performed on a Shimadzu HPLC using a C18 5 μm Gemini Phenomenex column, and an Rf-535 fluorescence detector, which was set to Ex 525 nm and EM 551 nm. The mobile phase consisted of a 60:40 (v/v) mixture of 10 mmol potassium dihydrogen phosphate (pH 6.8):methanol. MDA was

quantified by a calibration curve, which was constructed every day for analysis [30].

Real-Time Quantitative Reverse Transcription-Polymerase Chain Reaction (RT-PCR)

Gene expression of NADPH oxidase subunits (NOX2, NOX4, p22 phox, and p47 phox) and reference genes cyclophilin and glyceraldehyde-3-phosphate dehydrogenase (GAPDH) was analyzed by RT-PCR according to a previously described method [31]. Total RNA was extracted from LV myocardium with TRIzol Reagent (Invitrogen Life Technologies, Carlsbad, CA, USA) and treated with DNase I (Invitrogen Life Technologies). One microgram of RNA was reverse transcribed using High Capacity cDNA Reverse Transcription Kit, according to standard methods (Applied Biosystems, Foster City, CA, USA). Aliquots of cDNA were then submitted to real-time PCR reaction using a customized assay containing sense and antisense primers and Taqman (Applied Biosystems, Foster City, CA, USA) probes specific to each gene: NOX2 (Rn00576710 m1), NOX4 (Rn00585380 m1), p22 phox (Rn00577357 m1), and p47 phox (Rn00586945 m1). Amplification and analysis were performed using Step One Plus™ Real-Time PCR System (Applied Biosystems, Foster City, CA, USA). Expression data were normalized to reference gene expressions: cyclophilin (Rn00690933 m1) and GAPDH (Rn01775763 g1). Reactions were performed in triplicate and expression levels calculated using the CT comparative method ($2^{-\Delta\Delta CT}$).

Western blotting

Protein levels were analyzed by Western blotting as previously described [32, 33] using specific antibodies (Santa Cruz Biotechnology, Santa Cruz, CA, USA): total JNK1/2 (sc-137019), p-JNK (sc-6254), total p38-MAPK (sc-7972), p-p38-MAPK (sc-17852), total ERK 1 (sc-93), and p-ERK1/2 (sc-16982). Protein levels were normalized to GAPDH (6C5 sc-32233). Myocardial protein was extracted using RIPA buffer (containing proteases and phosphatases inhibitors); supernatant protein content was quantified by the Bradford method. Samples were separated

on a polyacrylamide gel and then transferred to a nitrocellulose membrane. After blockade, membrane was incubated with the primary antibodies. The membrane was then washed with TBS and Tween 20 and incubated with secondary peroxidase-conjugated antibodies. Super Signal ® West Pico Chemiluminescent Substrate (Pierce Protein Research Products, Rockford, USA) was used to detect bound antibodies.

Statistical analysis

Data are expressed as mean ± standard deviation or median and percentiles. Comparisons between groups were performed by one-way ANOVA and Tukey test or Kruskal-Wallis and Dunn test. Frequency of heart failure features was assessed by the Goodman test. Significance level was set at 5%.

Results

At the end of the experimental period, Sham group had 16 animals; one rat had ascites. AS and AS-NAC groups had 22 and 15 rats respectively. Heart failure feature frequencies are presented in Table 1. AS-NAC had a lower frequency of right ventricular hypertrophy than AS. Anatomical variables are shown in Table 2. Final body weight did not differ between groups. Absolute and normalized LV, right ventricle, atria, and lung weights were higher in AS and AS-NAC than Sham. Lung weight and lung weight-to-body weight ratio were higher in AS than Sham.

Before treatment, both aortic stenosis groups presented dilated left atrium and concentric LV hypertrophy with diastolic dysfunction and mild systolic dysfunction (Tables 3 and 4). Except for a lower systolic posterior wall thickness, AS-NAC did not differ from AS. At the end of the experiment, AS-NAC and AS preserved the same pattern of LV concentric hypertrophy and dysfunction. No differences were observed between AS-NAC and AS (Tables 5 and 6). However, TDI S', IVRT, and TDI E' were lower in AS than Sham; in AS-NAC, values for these parameters fell between those of the Sham and AS groups and did not significantly differ from either group.

Total glutathione was lower in AS than Sham and AS-NAC and reduced glutathione was lower in both AS and AS-NAC (Figure 1). Systemic and myocardial markers of oxidative stress were reduced in AS-NAC. Malondialdehyde serum concentration was lower in AS-NAC than Sham and AS. Lipid hydroperoxide myocardial concentration was lower in AS-NAC and Sham than AS (Figure 2). Antioxidant enzyme activities are shown in Figure 3. Superoxide dismutase was lower in AS and AS-NAC than Sham and glutathione peroxidase was lower in AS than Sham. Catalase activity did not differ between groups. NADPH oxidase subunit gene expression did not differ between groups (Table 7).

Myocyte diameter and interstitial collagen fraction were higher in AS than Sham and AS-NAC (Table 8). Myocardial MAPK protein expression is shown in Table 9. Phosphorylated-ERK/total ERK ratio was higher in AS than Sham and AS-NAC and p-JNK/GAPDH ratio was lower in AS-NAC than AS.

Table 1. Frequency of heart failure features (%)

	AS (n=22)	AS-NAC (n=15)
Ascites	59.1	46.7
Pleural effusion	27.3	13.3
Tachypnea	27.3	6.6
Atrial thrombi	36.4	26.6
Liver congestion	18.2	13.3
Lung congestion	59.1	40.0
Right ventricular hypertrophy	77.3	33.3 *

AS: aortic stenosis; AS-NAC: aortic stenosis treated with N-acetylcysteine; n: number of animals. Goodman test; * p < 0.05 vs AS.

Table 2. Anatomical data

	Sham (n=16)	AS (n=22)	AS-NAC (n=15)
BW (g)	510 ± 50.7	482 ± 41.6	490 ± 69.9
LVW (g)	0.94 (0.88-0.98)	1.84 (1.56-2.09)*	1.41 (1.09-1.56)*
LVW/BW (mg/g)	1.86 (1.69-2.05)	3.80 (2.98-4.33)*	2.82 (2.33-3.67)*
RVW (g)	0.24 (0.21-0.25)	0.46 (0.40-0.55)*	0.38 (0.25-0.49)*
RVW/BW (mg/g)	0.48 (0.45-0.50)	0.99 (0.83-1.11)*	0.76 (0.49-1.01)*
Atria weight (g)	0.10 (0.09-0.11)	0.36 (0.21-0.41)*	0.29 (0.17-0.40)*
Atria/BW (mg/g)	0.20 (0.19-0.23)	0.75 (0.66-0.82)*	0.61 (0.35-0.88)*
Lung weight (g)	1.80 (1.66-1.99)	2.89 (2.11-3.29)*	2.11 (1.57-3.12)
Lung/BW (mg/g)	3.80 (3.12-4.11)	6.30 (4.29-7.05)*	3.94 (3.34-6.12)

AS: aortic stenosis; AS-NAC: aortic stenosis treated with N-acetylcysteine; BW: body weight; LVW: left ventricle weight; RVW: right ventricle weight. One-way ANOVA and Tukey or Kruskal-Wallis and Dunn test. Data are mean ± SD or median and percentiles; $*$ p < 0.05 versus Sham.

Table 3. Echocardiographic structural data before treatment

	Sham (n=16)	AS (n=22)	AS-NAC (n=15)
BW (g)	472 ± 64.0	445 ± 33.2	488 ± 64.1
LVDD (mm)	8.03 ± 0.58	8.80 ± 0.74*	9.06 ± 0.84*
LVDD/BW (mm/kg)	17.2 ± 2.15	19.8 ± 1.68*	18.8 ± 2.36
LVSD (mm)	3.92 ± 0.57	4.10 ± 1.08	4.62 ± 1.12
DPWT (mm)	1.41 (1.37-1.44)	2.07 (1.90-2.22)*	2.07 (1.90-3.35)*
SPWT (mm)	2.91 ± 0.25	3.79 ± 0.53*	3.35 ± 0.34*#
DSWT (mm)	1.45 (1.40-1.49)	2.14 (1.82-2.18)*	1.94 (1.57-2.07)*
SSWT (mm)	2.49 (2.31-2.61)	3.11 (2.85-3.37)*	3.01 (2.81-3.14)*
RWT	0.34 (0.33-0.38)	0.46 (0.41-0.52)*	0.45 (0.41-0.47)*
AO (mm)	3.98 ± 0.28	3.88 ± 0.24	3.92 ± 0.20
LA (mm)	5.29 (5.11-6.08)	7.87 (6.31-8.58)*	8.54 (7.30-8.94)*
LA/AO	1.39 (1.32-1.43)	1.99 (1.56-2.31)*	1.84 (1.50-2.29)*
LA/BW (mm/kg)	11.4 (10.7-12.7)	18.4 (13.6-19.4)*	17.7 (13.8-19.1)*
LVM (g)	0.77 (0.72-0.88)	1.51 (1.25-1.78)*	1.65 (1.05-2.01)*
LVMI (g/kg)	1.71 (1.56-1.80)	3.45 (2.82-4.01)*	3.46 (2.54-4.28)*

AS: aortic stenosis; AS-NAC: aortic stenosis treated with N-acetylcysteine; BW: body weight; LVDD and LVSD: left ventricular (LV) diastolic and systolic diameters, respectively; DPWT and SPWT: LV diastolic and systolic posterior wall thickness, respectively; DSWT and SSWT: LV diastolic and systolic septal wall thickness, respectively; RWT: relative wall thickness; AO: aorta diameter; LA: left atrial diameter; LVM: LV mass; LVMI: LVM index. One-way ANOVA and Tukey or Kruskal-Wallis and Dunn test. Data are mean ± SD or median and percentiles; $* \ p < 0.05$ vs Sham; # $p < 0.05$ vs AS.

Table 4. Echocardiographic data of left ventricular function before treatment

	Sham (n=16)	AS (n=22)	AS-NAC (n=15)
HR (bpm)	261 ± 22.1	278 ± 37.6	295 ± 20.2*
EFS (%)	53.0 (47.7-56.3)	54.6 (45.3-60.4)	54.0 (44.0-58.6)
MFS (%)	31.0 ± 3.77	29.7 ± 6.43	30.2 ± 6.37
PWSV (mm/s)	39.3 (36.9-41.0)	30.3 (26.6-35.8)*	30.4 (25.9-36.0)*
Tei index	0.46 ± 0.07	0.45 ± 0.09	0.45 ± 0.08
EF	0.89 (0.84-0.91)	0.91 (0.86-0.94)	0.87 (0.80-0.91)
TDI S' (average, cm/s)	3.47 ± 0.43	2.83 ± 0.49*	3.17 ± 0.62
Mitral E (cm/s)	78.0 (70.3-81.5)	127 (93.5-149)*	140 (100-157)*
Mitral A (cm/s)	50.5 (46.3-55.5)	29.0 (18.5-57.0)	53.0 (25.0-64.0)
E/A	1.52 ± 0.19	4.92 ± 3.70*	3.58 ± 3.14
IVRT (ms)	26.0 (23.0-27.5)	18.0 (15.0-26.0)*	15.0 (15.0-20.0)*
IVRTn (ms)	53.1 (48.8-57.5)	41.5 (32.3-53.7)*	34.9 (30.8-43.2)*
EDT (ms)	47.5 (41.7-56.0)	30.0 (26.0-48.0)*	30.0 (27.5- 36.0)*
TDI E' (average, cm/s)	4.16 ± 0.68	3.82 ± 093	4.09 ± 0.67
TDI A' (average, cm/s)	3.20 (2.86-3.56)	3.23 (2.73-3.81)	3.35 (3.15-4.45)
E/TDI E' (average)	19.0 (16.5-22.2)	36.2 (27.6-39.7)*	25.4 (19.4-37.5)*

AS: aortic stenosis; AS-NAC: aortic stenosis treated with N-acetylcysteine; HR: heart rate; EFS: endocardial fractional shortening; MFS: midwall fractional shortening; PWSV: posterior wall shortening velocity; Tei index: myocardial performance index; EF: ejection fraction; TDI S': tissue Doppler imaging (TDI) of systolic velocity of the mitral annulus; E/A: ratio between early (E)-to-late (A) diastolic mitral inflow; IVRT: isovolumetric relaxation time; IVRTn: IVRT normalized to heart rate; EDT: E wave deceleration time; TDI E' and A': TDI of early (E') and late (A') diastolic velocity of mitral annulus. One-way ANOVA and Tukey or Kruskal-Wallis and Dunn test. Data are mean ± SD or median and percentiles; * $p < 0.05$ vs Sham.

Table 5. Echocardiographic structural data after treatment

	Sham (n=16)	AS (n=22)	AS-NAC (n=15)
BW (g)	510 ± 50.7	482 ± 41.6	490 ± 69.9
LVDD (mm)	8.31 ± 0.57	9.02 ± 0.90*	9.07 ± 0.95*
LVDD/BW (mm/kg)	16.8 ± 2.20	18.9 ± 2.65	18.5 ± 3.24
LVSD (mm)	4.02 (3.58-4.58)	4.80 (3.66-5.29)	4.67 (3.82-5.29)
DPWT (mm)	1.42 (1.38-1.45)	2.06 (1.87-2.12)*	1.94 (1.57-2.07)*
SPWT (mm)	2.99 ± 0.31	3.47 ± 0.51*	3.48 ± 0.42*
DSWT (mm)	1.42 (1.38-1.46)	2.11 (1.87-2.16)*	1.94 (1.57-2.11)*
SSWT (mm)	2.53 (2.42-2.68)	2.90 (2.64-3.21)*	3.01 (2.68-3.26)*
RWT	0.34 (0.33-0.36)	0.43 (0.39-0.51)*	0.44 (0.36-0.47)*
AO (mm)	3.98 ± 0.20	4.00 ± 0.25	4.08 ± 0.23
LA (mm)	5.29 (4.93-5.69)	8.36 (7.55-8.71)*	7.48 (6.15-9.26)*
LA/AO	1.36 (1.26-1.44)	2.17 (1.74-2.29)*	1.84 (1.54-2.49)*
LA/BW (mm/kg)	10.5 (9.71-12.4)	17.3 (14.7-19.5)*	17.5 (13.7-19.0)*
LVM (g)	0.81 (0.76-0.88)	1.47 (1.34-1.94)*	1.13 (0.97-2.06)*
LVMI (g/kg)	1.65 (1.40-1.77)	3.01 (2.69-3.99)*	2.72 (2.06-4.01)*

AS: aortic stenosis; AS-NAC: aortic stenosis treated with N-acetylcysteine; BW: body weight; LVDD and LVSD: left ventricular (LV) diastolic and systolic diameters, respectively; DPWT and SPWT: LV diastolic and systolic posterior wall thickness, respectively; DSWT and SSWT: LV diastolic and systolic septal wall thickness, respectively; RWT: relative wall thickness; AO: aorta diameter; LA: left atrial diameter; LVM: LV mass; LVMI: LVM index. One-way ANOVA and Tukey or Kruskal-Wallis and Dunn test. Data are mean ± SD or median and percentiles; $* \ p < 0.05$ vs Sham.

Table 6. Echocardiographic data of left ventricular function after treatment

	Sham (n=16)	AS (n=22)	AS-NAC (n=15)
HR (bpm)	295 ± 44.4	292 ± 40.1	294 ± 19.2
EFS (%)	51.6 (46.4-55.2)	49.0 (41.8-55.3)	53.2 (44.0-61.8)
MFS (%)	28.7 (26.5-32.4)	30.2 (21.2-35.6)	30.4 (24.6-36.5)
PWSV (mm/s)	39.3 (36.8-41.0)	30.3 (26.6-35.8)*	30.2 (24.5-40.4)*
Tei index	0.39 (0.37-0.45)	0.41 (0.38-0.50)	0.45 (0.42-0.52)
EF	0.89 (0.85-0.91)	0.91 (0.86-0.94)	0.85 (0.82-0.92)
TDI S' (average, cm/s)	4.03 ± 0.64	2.89 ± 0.64*	3.15± 0.60
Mitral E (cm/s)	77.5 (70.5-86.5)	141 (89.7-161)*	122 (85.0-142)*
Mitral A (cm/s)	59.5 (50.0-69.3)	27.0 (22.0-53.5)*	36.0 (22.0-57.0)*
E/A	1.35 (1.15-1.58)	5.38 (1.73-7.37)*	3.88 (1.70-8.47)*
IVRT (ms)	52.6 (48.3-55.3)	40.8 (33.6-51.6)*	48.5 (37.2-53.1)
IVRTn	55.2 (49.0-60.4)	39.2 (33.6-45.9)*	40.7 (32.4-47.1)*
EDT (ms)	44.0 (41.0-51.0)	30.0 (24.0-40.0)*	33.0 (30.0-41.0)*
TDI E' (average, cm/s)	4.70 (4.26-5.21)	3.80 (3.30-4.90)*	4.00 (3.74-4.53)
TDI A' (average, cm/s)	4.38 (3.76-6.04)	3.55 (2.90-4.75)	3.05 (2.40-3.45)*
E/TDI E' (average)	17.5 (13.6-18.8)	35.0 (27.4-41.9)*	30.2 (18.9-37.9)*

AS: aortic stenosis; AS-NAC: aortic stenosis treated with N-acetylcysteine; HR: heart rate; EFS: endocardial fractional shortening; MFS: midwall fractional shortening; PWSV: posterior wall shortening velocity; Tei index: myocardial performance index; EF: ejection fraction; TDI S': tissue Doppler imaging (TDI) of systolic velocity of the mitral annulus; E/A: ratio between early (E)-to-late (A) diastolic mitral inflow; IVRT: isovolumetric relaxation time; IVRTn: IVRT normalized to heart rate; EDT: E wave deceleration time; TDI E' and A': TDI of early (E') and late (A') diastolic velocity of mitral annulus. One-way ANOVA and Tukey or Kruskal-Wallis and Dunn test. Data are mean ± SD or median and percentiles; * $p < 0.05$ vs Sham.

Table 7. Myocardial gene expression of NADPH oxidase subunits

	Sham (n=8)	AS (n=6)	AS-NAC (n=8)
p22 phox	1.00 ± 0.51	1.26 ± 0.98	0.92 ± 0.14
p47 phox	1.04 ± 0.50	0.89 ± 0.61	0.83 ± 0.71
NOX 2	0.74 ± 0.55	1.64 ± 0.29	0.66 ± 0.43
NOX 4	1.00 ± 0.85	3.47 ± 0.19	1.16 ± 0.66

AS: aortic stenosis; AS-NAC: aortic stenosis treated with N-acetylcysteine. One-way ANOVA and Tukey test. Data are mean ± SD.

Table 8. Myocardial morphometric parameters

	Sham (n=10)	AS (n=12)	AS-NAC (n=8)
Myocyte diameter (μm)	13.4 ± 1.17	15.1 ± 0.87*	14.6 ± 1.19#
ICF (%)	4.30 ± 1.20	9.86 ± 1.69*	4.77 ± 1.66#

AS: aortic stenosis; AS-NAC: aortic stenosis treated with N-acetylcysteine; ICF: interstitial collagen fraction. One-way ANOVA and Tukey test. Data are mean ± SD; * $p < 0.05$ vs Sham; # $p < 0.05$ vs AS.

Table 9. Myocardial expression of MAPK proteins

		Sham (n=7)	AS (n=7)	AS-NAC (n=7)
ERK	p-ERK/ERK	1.00 ± 0.22	1.46 ± 0.34*	0.97 ± 0.31#
	p-ERK/GAPDH	1.00 ± 0.16	1.30 ± 0.85	1.22 ± 0.50
	ERK/GAPDH	1.00 ± 0.21	0.98 ± 0.41	1.13 ± 0.22
JNK	p-JNK/JNK	1.01 (0.86-1.07)	0.78 (0.68-1.27)	0.78 (0.55-1.27)
	p-JNK/GAPDH	1.07 (0.95-1.18)	1.15 (0.92-1.26)	0.83 (0.62-1.45)#
	JNK/GAPDH	1.00 ± 0.23	1.11 ± 0.19	0.95 ± 0.40
P38	p-P38/P38	0.74 (0.50-1.68)	1.29 (1.23-1.81)	0.70 (0.57-1.04)
	p-P38/GAPDH	1.00 ± 0.54	2.01 ± 1.30	1.47 ± 0.69
	P38/GAPDH	1.05 (0.81-1.13)	1.00 (0.70-2.58)	1.49 (0.99-2.86)

AS: aortic stenosis; AS-NAC: aortic stenosis treated with N-acetylcysteine. One-way ANOVA and Tukey or Kruskal-Wallis and Dunn test. Data are mean ± SD or median and percentiles; * $p < 0.05$ vs Sham; # $p < 0.05$ vs AS.

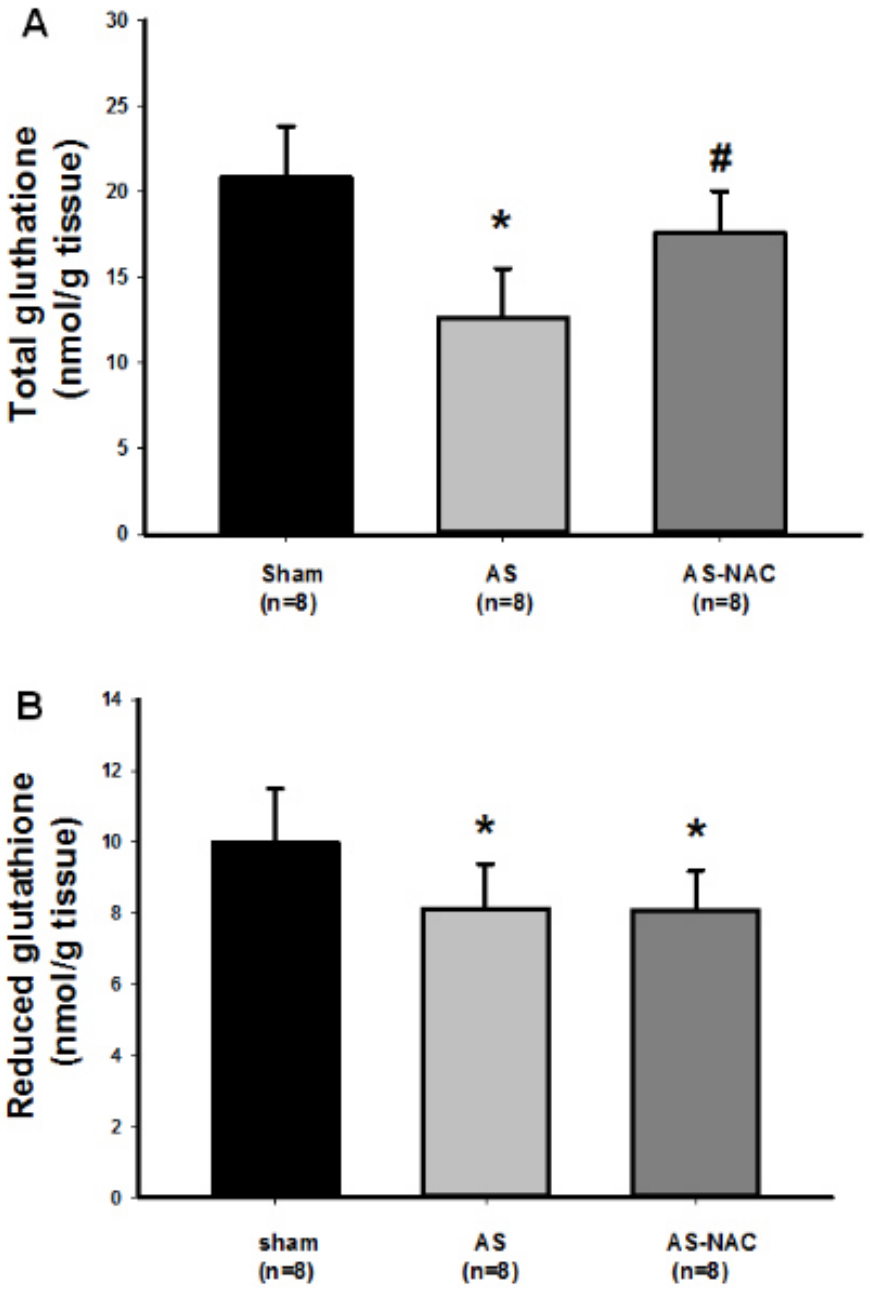

Figure 1: Myocardial concentration of total (A) and reduced glutathione (B). AS: aortic stenosis; AS-NAC: aortic stenosis treated with *N*-acetylcysteine; n: number of animals. Data are mean ± SD; ANOVA and Tukey; * $p < 0.05$ vs Sham; # $p < 0.05$ vs AS.

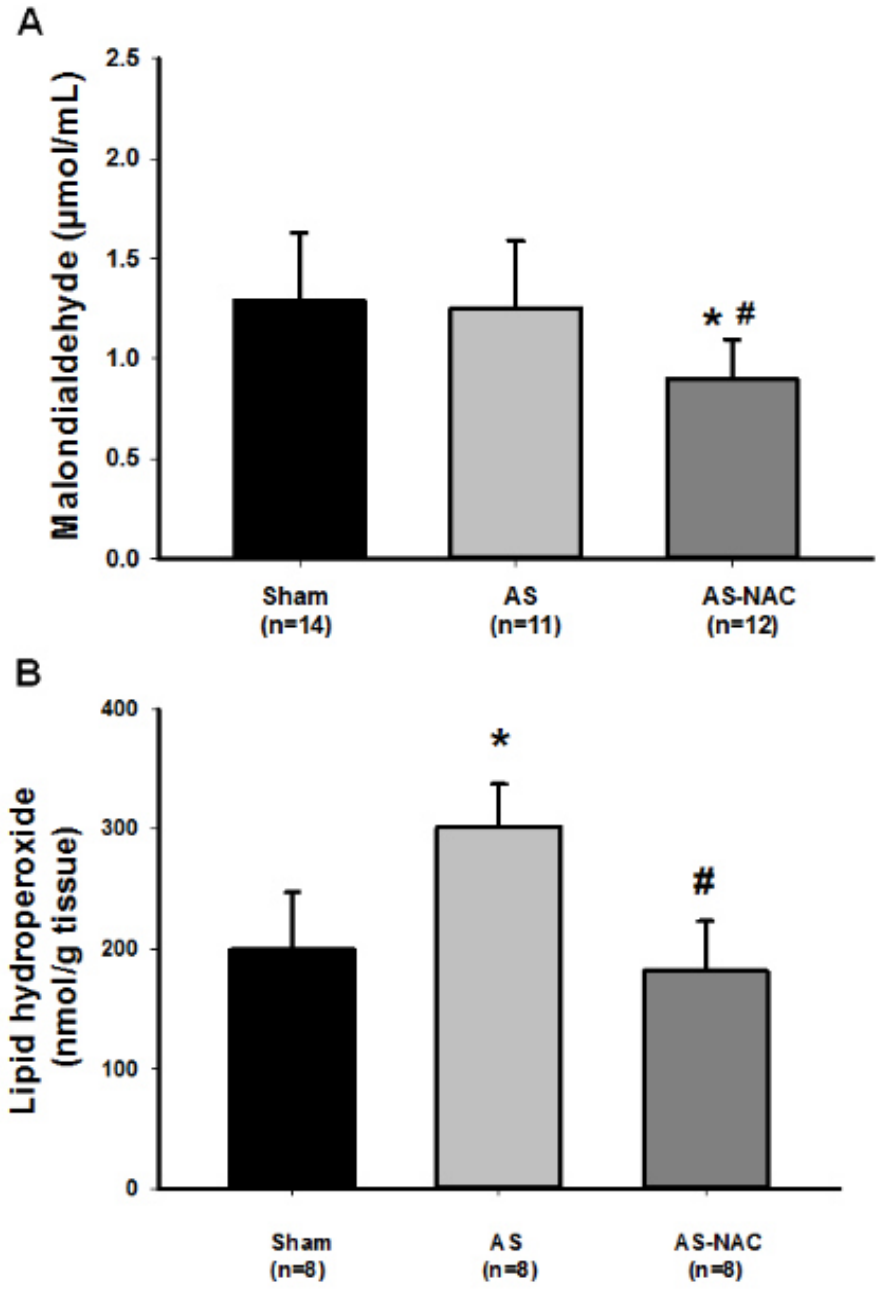

Figure 2: Malondialdehyde serum concentration (A) and lipid hydroperoxide myocardial concentration (B). AS: aortic stenosis; AS-NAC: aortic stenosis treated with *N*-acetylcysteine; n: number of animals. Data are mean ± SD; ANOVA and Tukey; * $p < 0.05$ vs Sham; # $p < 0.05$ vs AS.

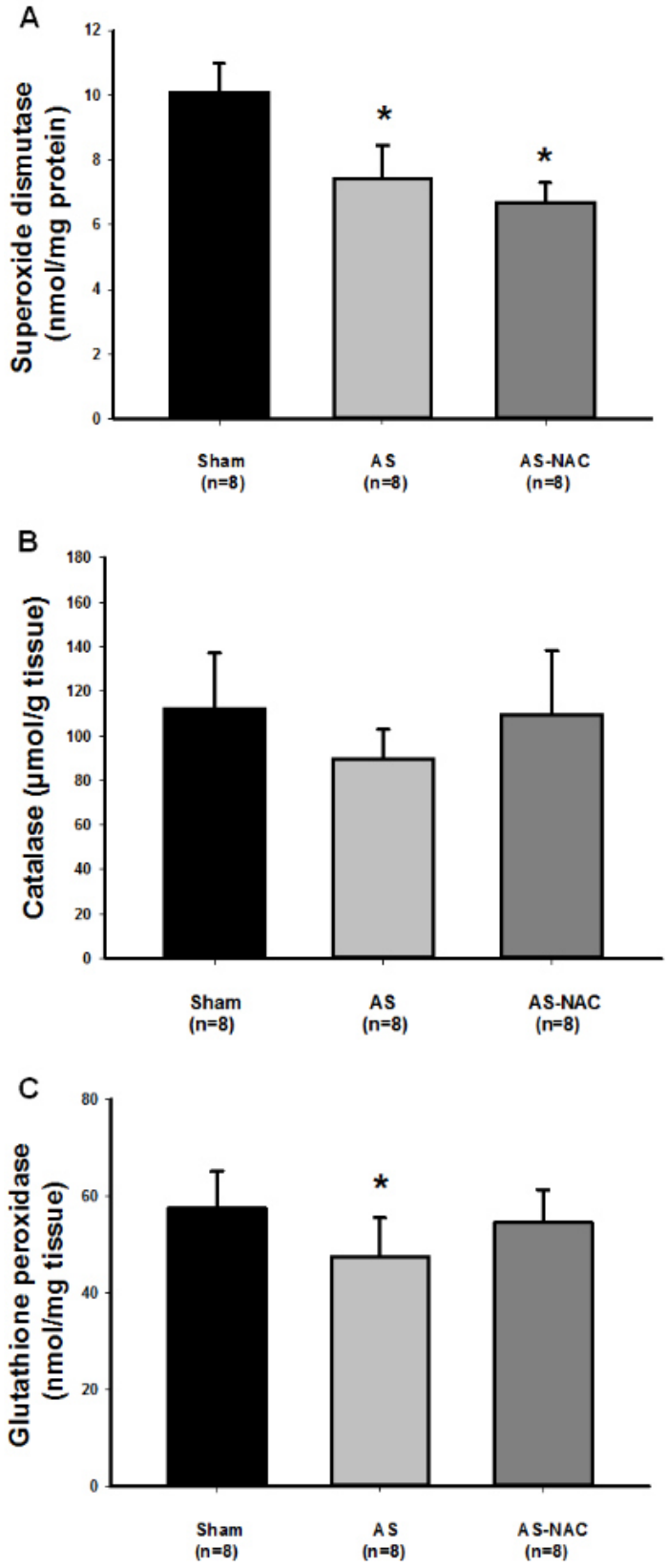

Figure 3. Antioxidant enzyme activity in myocardium. (A): superoxide dismutase; (B): catalase; (C): glutathione peroxidase. AS: aortic stenosis; AS-NAC: aortic stenosis treated with *N*-acetylcysteine; n: number of animals. Data are mean ± SD; ANOVA and Tukey; * $p < 0.05$ vs Sham.

Discussion

In this study, the effects of NAC were evaluated in aortic stenosis rats during the transition from LV compensated hypertrophy to overt heart failure.

Aortic stenosis in young rats has been often used to evaluate persistent pressure overload from early LV concentric hypertrophy through gradual LV dysfunction and decompensated heart failure [16]. After aortic stenosis induction, rats remain compensated for approximately 20 to 28 weeks [34]. They then begin to present clinical and pathological heart failure features and evolve to death within two to four weeks. In this study, after a chronic period of LV hypertrophy, rats were randomly distributed into different treatment groups. Cardiac structures and LV function were evaluated by transthoracic echocardiogram before and after NAC treatment. The presence of cardiac failure was demonstrated by the high frequency of heart failure features observed at euthanize in the AS group.

Before treatment, aortic stenosis rats had concentric LV hypertrophy characterized by an increase in LV mass, LV wall thicknesses, and relative wall thickness. Mild systolic dysfunction was characterized by reduced posterior wall shortening velocity, and diastolic dysfunction by increased E wave and E/TDI E' ratio, and reduced isovolumetric relaxation time (IVRT) and E wave deceleration time. At the end of the experiment, both AS and AS-NAC preserved the same pattern of cardiac remodeling. However, the AS group had an impairment in TDI S', an index of systolic function, and in IVRT and TDI E', which evaluates diastolic function, compared to the Sham group. Values of these parameters in AS-NAC fell between those of the Sham and AS groups and did not significantly differ from either group. These results suggest that NAC administration may have attenuated LV dysfunction. This may be reinforced by the fact that AS-NAC had a lower frequency of right ventricular hypertrophy than AS, a later event in LV pressure overload [35].

NAC is a precursor to an important intracellular defense mechanism against oxidative damage. By providing cysteine to glutathione synthesis, NAC replenishes glutathione, which is usually depleted in several disease states [12]. The replenishment of glutathione in deficient cells plays a central role in the effects of NAC as an antioxidant agent [10]. In fact, NAC is probably ineffective in cells

replete in glutathione [10]. This property is important for antioxidant agents because at appropriate concentrations, reactive oxygen species also have fundamental roles in cellular function [8, 36].

In this study, we first analyzed myocardial glutathione status. Total glutathione was decreased in AS and normalized by NAC. However, reduced glutathione was decreased in AS and AS-NAC groups. Depleted cardiac total glutathione has been previously observed in both congestive heart failure patients and post-myocardial infarction rats, as has total glutathione repletion after NAC treatment in infarcted rats [11]. We next evaluated systemic and myocardial markers of oxidative stress and myocardial antioxidant enzyme activity. Myocardial oxidative stress, analyzed by lipid hydroperoxide concentration, was higher in AS and normalized by NAC. Interestingly, malondialdehyde serum concentration was decreased in AS-NAC compared to both Sham and AS groups. As total glutathione was replenished in AS-NAC, glutathione peroxidase activity was normalized and its ability to neutralize free radicals increased, resulting in reduced lipoperoxidation. Therefore, NAC administration restored myocardial total glutathione and glutathione peroxidase activity, and reduced myocardial and systemic oxidative stress markers.

The NADPH oxidase family, composed of enzymes whose main function is producing reactive oxygen species, is involved in the pathophysiology of several cardiovascular diseases [5, 6, 37]. To evaluate the potential role of NADPH oxidase on increased oxidative stress, we assessed gene expression NOX2 and NOX4 - the main cardiac isoforms, p22 phox - the transmembrane protein, and p47 phox - the NOX2 cytosolic regulatory subunit, all which did not differ between groups. However, as we did not evaluate NADPH oxidase activity, we cannot discard the possible influence of NADPH oxidase on increased oxidative stress in the AS group. We have previously observed that NAC administration decreases NADPH oxidase activity and NOX4 and p22 phox gene expression in the soleus muscle of heart failure rats [38].

Experimental studies have shown that the mitogen-activated protein kinase (MAPK) signaling pathway is involved in myocardial response to oxidative stress in several conditions [39-41]. MAPK includes four subfamilies, three of which

have been well characterized: extracellular regulated kinase (ERK 1/2), c-jun N-terminal kinase (JNK), and p38-MAPK. After oxidative stress increase, MAPK downstream signaling may lead to myocardial hypertrophy and fibrosis [6, 39, 40, 42]. We therefore evaluated MAPK protein expression and observed that p-ERK and p-JNK were lower in AS-NAC than AS. Probably as a consequence of the reduced oxidative stress and p-ERK and p-JNK signaling, myocyte hypertrophy and myocardial fibrosis were attenuated by NAC treatment. As myocardial hypertrophy and fibrosis are strongly related to poor outcome in cardiovascular diseases [2, 43], these results are important for future clinical studies.

More recently, NAC has been evaluated in experimental models of cardiac injury, particularly hypertrophic cardiomyopathy in which NAC reduced oxidative stress, reversed established cardiac hypertrophy and fibrosis, prevented cardiac systolic and diastolic dysfunction, and improved arrhythmogenic propensity [12, 14, 44]. Similarly to our findings, NAC also reduced ERK and JNK phosphorylation [14, 44]. The antifibrotic effect of NAC was also observed in other models and organs [44, 46]. Despite the well characterized actions of NAC on hypertrophic cardiomyopathy, its effects on aortic stenosis-induced cardiac remodeling have been poorly addressed. When administered before and after aortic stenosis induction surgery, NAC attenuated increased LV weight and electrical remodeling [15]. On the other hand, NAC did not improve cardiac function in aortic stenosis mice [47].

We have therefore shown for the first time that antioxidant NAC restores myocardial total glutathione and reduces systemic and myocardial oxidative stress. Probably, as a consequence of this decreased oxidative stress, myocardial MAPK signaling was improved and myocardial hypertrophy and fibrosis were attenuated. However, cardiac echocardiographic parameters and heart failure features were only marginally improved. NAC administration was probably initiated too late when rats had already presented advanced degrees of structural cardiac alterations, thus preventing a reverse remodeling process. Our results therefore allow us to propose the hypothesis that early administration of NAC may be a useful treatment for preventing pathological cardiac remodeling and LV dysfunction during persistent LV pressure overload.

In conclusion, *N*-acetylcysteine treatment restores myocardial total glutathione, reduces systemic and myocardial oxidative stress, improves MAPK signaling, and attenuates myocyte hypertrophy, myocardial fibrosis, and left ventricular dysfunction in aortic stenosis rats during transition from compensated left ventricular hypertrophy to heart failure.

Acknowledgments

The authors are grateful to Jose Carlos Georgette for their technical assistance and Colin Edward Knaggs for English editing. Financial support was provided by CNPq (Proc. n. 306770/2015-6 and 308674/2015-4), FAPESP (Proc. n. 2015/17539-5), CAPES, PROPe, UNESP, and PAEDEX/AUIP Program.

Disclosures

The authors declare that there are no conflicts of interest regarding the publication of this article.

References

1. Drazner MH. The progression of hypertensive heart disease. Circulation 2011; 123: 327-334.

2. Crozatier B, Ventura-Clapier R. Inhibition of hypertrophy, per se, may not be a good therapeutic strategy in ventricular pressure overload: other approaches could be more beneficial. Circulation 2015; 131: 1448-1457.

3. Schiattarella GG, Hill JA. Inhibition of hypertrophy is a good therapeutic strategy in ventricular pressure overload. Circulation 2015; 131: 1435-1447.

4. Zwadlo C, Schmidtmann E, Szaroszyk M, Kattih B, Froese N, Hinz H, et al. Antiandrogenic therapy with finasteride attenuates cardiac hypertrophy and left ventricular dysfunction. Circulation 2015; 131: 1071-1081.

5. Sag CM, Santos CX, Shah AM. Redox regulation of cardiac hypertrophy. J Mol Cell Cardiol 2014; 73: 103-111.

6. Madamanchi NR, Runge MS. Redox signaling in cardiovascular health and disease. Free Rad Biol Med 2013; 61: 473-501.

7. Munzel T, Gori T, Keaney Jr JF, Maack C, Daiber A. Pathophysiological role of oxidative stress in systolic and diastolic heart failure and its therapeutic implications. Eur Heart J 2015; 36: 2555-2564.

8. Altenhofer S, Radermacher KA, Kleikers PW, Wingler K, Schmidt HH. Evolution of NADPH oxidase inhibitors: selectivity and mechanisms for target engagement. Antioxid Redox Signal 2015; 23: 406-427.

9. Fratelli M, Goodwin LO, Orom UA, Lombardi S, Tonelli R, Mengozzi M, Ghezzi P. Gene expression profiling reveals a signaling role of glutathione in redox regulation. Proc Natl Acad Sci U S A 2005; 102: 13998-14003.

10. Rushworth GF, Megson IL. Existing and potential therapeutic uses for N-acetylcysteine: the need for conversion to intracellular glutathione for antioxidant benefits. Pharmacol Ther 2014; 141: 150-159.

11. Adamy C, Mulder P, Khouzami L, Andrieu-Abadie N, Defer N, Candiani G, et al. Neutral sphingomyelinase inhibition participates to the benefits of N-

acetylcysteine treatment in post-myocardial infarction failing heart rats. J Mol Cell Cardiol 2007; 43: 344-353.

12. Lombardi R, Rodriguez G, Chen SN, Ripplinger CM, Li W, Chen J, et al. Resolution of established cardiac hypertrophy and fibrosis and prevention of systolic dysfunction in a transgenic rabbit model of human cardiomyopathy through thiol-sensitive mechanisms. Circulation 2009; 119: 1398-1407.

13. Giam B, Chu PY, Kuruppu S, Smith AI, Horlock D, Kiriazis H, et al. N-acetylcysteine attenuates the development of cardiac fibrosis and remodeling in a mouse model of heart failure. Physiol Rep 2016; 4: e12757.

14. Wilder T, Ryba DM, Wieczorek DF, Wolska BM, Solaro RJ. N-acetylcysteine reverses diastolic dysfunction and hypertrophy in familial hypertrophic cardiomyopathy. Am J Physiol Heart Circ Physiol 2015; 309: H1720-H1730.

15. Foltz WU, Wagner M, Rudakova E, Volk T. N-acetylcysteine prevents electrical remodeling and attenuates cellular hypertrophy in epicardial myocytes of rats with ascending aortic stenosis. Basic Res Cardiol 2012; 107: 290.

16. Gomes MJ, Martinez PF, Campos DHS, Pagan LU, Bonomo C, Lima AR, et al. Beneficial effects of physical exercise on functional capacity and skeletal muscle oxidative stress in rats with aortic stenosis-induced heart failure. Oxid Med Cell Longev 2016; 2016: 8695716.

17. Moreira VO, Pereira CA, Silva MO, Felisbino SL, Cicogna AC, Okoshi K, et al. Growth hormone attenuates myocardial fibrosis in rats with chronic pressure overload-induced left ventricular hypertrophy. Clin Exp Pharmacol Physiol 2009; 36: 325-330.

18. Damatto RL, Martinez PF, Lima AR, Cezar MD, Campos DH, Oliveira SAJ, et al. Heart failure-induced skeletal myopathy in spontaneously hypertensive rats. Int J Cardiol 2013; 167: 698-703.

19. Martinez PF, Okoshi K, Zornoff LA, Carvalho RF, Oliveira Junior SA, Lima AR, et al. Chronic heart failure-induced skeletal muscle atrophy, necrosis, and myogenic regulatory factors changes. Med Sci Monit 2010; 16: 374-383.

20. Okoshi K, Fioretto JR, Okoshi MP, Cicogna AC, Aragon FF, Matsubara LS, et al. Food restriction induces in vivo ventricular dysfunction in spontaneously hypertensive rats without impairment of in vitro myocardial contractility. Braz J Med Biol Res. 2004;37:607-613.

21. Oliveira Junior SA, Dal Pai-Silva M, Martinez PF, Lima-Leopoldo AP, Campos DH, Leopoldo AS, et al. Diet-induced obesity causes metabolic, endocrine and cardiac alterations in spontaneously hypertensive rats. Med Sci Monit 2010; 16: BR367-BR373.

22. Oliveira-Junior SA, Martinez PF, Fan WYC, Nakatani BT, Pagan LU, Padovani CR, et al. Association between echocardiographic structural parameters and body weight in Wistar rats. Oncotarget 2017; 8: 26100-26105.

23. Pagan LU, Damatto RL, Cezar MD, Lima AR, Bonomo C, Campos DH, et al. Long-term low intensity physical exercise attenuates heart failure development in aging spontaneously hypertensive rats. Cell Physiol Biochem 2015; 36: 61-74.

24. Lima AR, Martinez PF, Damatto RL, Cezar MD, Guizoni DM, Bonomo C, et al. Heart failure-induced diaphragm myopathy. Cell Physiol Biochem 2014; 34: 333-345.

25. Guizoni DM, Oliveira-Junior SA, Noor SL, Pagan LU, Martinez PF, Lima AR, et al. Effects of late exercise on cardiac remodeling and myocardial calcium handling proteins in rats with moderate and large size myocardial infarction. Int J Cardiol 2016; 221: 406-412.

26. Matsubara LS, Matsubara BB, Okoshi MP, Franco M, Cicogna AC. Myocardial fibrosis rather than hypertrophy induces diastolic dysfunction in renovascular hypertensive rats. Can J Physiol Pharmacol 1997; 75: 1328-1334.

27. Tietze F. Enzymic method for quantitative determination of nanogram amounts of total and oxidized glutathione: applications to mammalian blood and other tissues. Anal Biochem 1969; 27: 502-522.

28. Rosa CM, Gimenes R, Campos DH, Guirado GN, Gimenes C, Fernandes AA, et al. Apocynin influence on oxidative stress and cardiac remodeling of

spontaneously hypertensive rats with diabetes mellitus. Cardiovasc Diabetol 2016; 15: 126.

29. Gimenes C, Gimenes R, Rosa CM, Xavier NP, Campos DHS, Fernandes AAH, et al. Low intensity physical exercise attenuates cardiac remodeling and myocardial oxidative stress and dysfunction in diabetic rats. J Diabetes Res 2015: ID457848.

30. Nielsen F, Mikkelsen BB, Nielsen JB, Andersen HR, Grandjean P. Plasma malondialdehyde as biomarker for oxidative stress: reference interval and effects of life-style factors. Clin Chem 1997; 43: 1209-1214.

31. Cezar MD, Damatto RL, Martinez PF, Lima AR, Campos DH, Rosa CM, et al. Aldosterone blockade reduces mortality without changing cardiac remodeling in spontaneously hypertensive rats. Cell Physiol Biochem 2013; 32: 1275-1287.

32. Cezar MD, Damatto RL, Pagan LU, Lima AR, Martinez PF, Bonomo C, et al. Early spironolactone treatment attenuates heart failure development by improving myocardial function and reducing fibrosis in spontaneously hypertensive rats. Cell Physiol Biochem 2015; 36: 1453-1466.

33. Oliveira-Junior SA, Martinez PF, Guizoni DM, Campos DH, Fernandes T, Oliveira EM, et al. AT1 receptor blockade attenuates insulin resistance and myocardial remodeling in rats with diet-induced obesity. PLoS One 2014; 9: e86447.

34. Okoshi MP, Cezar MD, Iyomasa RM, Silva MB, Costa LC, Martinez PF, et al. Effects of early aldosterone antagonism on cardiac remodeling in rats with aortic stenosis-induced pressure overload. Int J Cardiol 2016; 222: 569-575.

35. Damatto RL, Lima AR, Martinez PF, Cezar MD, Okoshi K, Okoshi MP. Myocardial myostatin in spontaneously hypertensive rats with heart failure. Int J Cardiol 2016; 215: 384-387.

36. Arcaro A, Pirozzi F, Angelini A, Chimenti C, Crotti L, Giordano C, et al. Novel perspectives in redox biology and pathophysiology of failing myocytes: modulation of the intramyocardial redox milieu for therapeutic interventions

- a review article from the Working Group of Cardiac Cell Biology, Italian Society of Cardiology. Oxid Med Cell Longev 2016; 2016: 6353469.

37. Cao TT, Chen HH, Dong Z, Xu YW, Zhao P, Guo W, et al. Stachydrine protects against pressure overload-induced cardiac hypertrophy by suppressing autophagy. Cell Physiol Biochem 2017; 42: 103-114.

38. Martinez PF, Bonomo C, Guizoni DM, Junior SA, Damatto RL, Cezar MD, et al. Influence of N-acetylcysteine on oxidative stress in slow-twitch soleus muscle of heart failure rats. Cell Physiol Biochem 2015; 35: 148-159.

39. Suchal K, Malik S, Gamad N, Malhotra RK, Goyal SN, Chaudhary U, et al. Kaempferol attenuates myocardial ischemic injury via inhibition of MAPK signaling pathway in experimental model of myocardial ischemia-reperfusion injury. Oxid Med Cell Longev 2016; 2016: 7580731.

40. Xu Z, Sun J, Tong Q, Lin Q, Qian L, Park Y, et al. The role of ERK1/2 in the development of diabetic cardiomyopathy. Int J Mol Sci 2016; 17: E2001.

41. Martinez PF, Bonomo C, Guizoni DM, Junior SA, Damatto RL, Cezar MD, et al. Modulation of MAPK and NF-kappab signaling pathways by antioxidant therapy in skeletal muscle of heart failure rats. Cell Physiol Biochem 2016; 39: 371-384.

42. Ren J, Zhang N, Liao H, Chen S, Xu L, Li J, et al. Caffeic acid phenethyl ester attenuates pathological cardiac hypertrophy by regulation of MEK/ERK signaling pathway in vivo and vitro. Life Sci 2017: in press.

43. Roe AT, Aronsen JM, Skardal K, Hamdani N, Linke WA, Danielsen HE, et al. Increased passive stiffness promotes diastolic dysfunction despite improved Ca^{2+} handling during left ventricular concentric hypertrophy. Cardiovasc Res 2017: in press.

44. Marian AJ, Senthil V, Chen SN, Lombardi R. Antifibrotic effects of antioxidant N-acetylcysteine in a mouse model of human hypertrophic cardiomyopathy mutation. J Am Coll Cardiol 2006; 47: 827-834.

45. Demedts M, Behr J, Buhl R, Costabel U, Dekhuijzen R, Jansen HM, et al. IFIGENIA Study Group. High-dose acetylcysteine in idiopathic pulmonary fibrosis. N Engl J Med 2005; 353: 2229-2242.

46. Liu RM, Liu Y, Forman HJ, Olman M, Tarpey MM. Glutathione regulates transforming growth factor-beta-stimulated collagen production in fibroblasts. Am J Physiol Lung Cell Mol Physiol 2004; 286: L121-L128.

47. van Deel ED, Octavia Y, de Boer M, Juni RP, Tempel D, van Haperen R, et al. Normal and high eNOS levels are detrimental in both mild and severe cardiac pressure-overload J Mol Cell Cardiol 2015; 88: 145-154.

EXERCISE DURING TRANSITION FROM COMPENSATED LEFT VENTRICULAR HYPERTROPHY TO HEART FAILURE IN AORTIC STENOSIS RATS

David RA Reyes[1], Mariana J Gomes[1], Camila M Rosa[1], Luana U Pagan[1], Felipe C Damatto[1], Ricardo L Damatto[1], Dijon HS Campos[1], Eder A Rodrigues[1], Robson F Carvalho[2], Ana AH Fernandez[2], Paula F Martinez[3], Aline RR Lima[1], Marcelo DM Cezar[1], Katashi Okoshi[1], Marina P Okoshi[1]

[1] Department of Internal Medicine, Botucatu Medical School, Sao Paulo State University, UNESP, Botucatu, SP, Brazil

[2] Botucatu Institute of Biosciences, Sao Paulo State University, UNESP, Botucatu, SP, Brazil

[3] Federal University of Mato Grosso do Sul, Campo Grande, MS, Brasil

Correspondence author: Marina P Okoshi

Address: Faculdade de Medicina de Botucatu, Departamento de Clinica Medica. Rubiao Junior, S/N CEP 18.618-687 Botucatu, SP, Brazil

e-mail: mpoliti@fmb.unesp.br

Introduction

Pathological cardiac hypertrophy induced by chronic pressure overload conditions, such as aortic stenosis and arterial systemic hypertension, is often associated with impaired prognosis and increased mortality [1]. Long-term pressure overload is a major cause of cardiac remodeling evolving progressively from compensated left ventricular hypertrophy to diastolic and systolic dysfunction and clinical heart failure [2].

Despite advances in the pharmacologic treatment of heart failure, its morbidity and mortality remain elevated [1]. Current guidelines strongly recommend physical exercise for patients with stable heart failure to prevent and/or attenuate cardiac remodeling and skeletal muscle changes and to improve functional capacity and quality of life [3-7]. In experimental heart failure, physical exercise attenuated ventricular dilation, cardiac dysfunction, increased passive stiffness, myocyte hypertrophy, myocardial fibrosis, myocyte calcium handling changes, and mitochondrial dysfunction [8-17]. However, as most benefits of exercise have been described in experimental models of myocardial infarction-induced heart failure [18], the effects of exercise during sustained left ventricular pressure-overload remains poorly understood. In fact, studies performed in this experimental model have observed controversial results. Aortic stenosis mice subjected to an eight-week period of voluntary rotating wheel exercise had no improvement in left ventricular function and presented a trend towards impaired ventricular dysfunction in severe cases [19]. As mice perform very well in voluntary wheel running [20], it is possible that excessive exercise might have contributed to these results [19]. In fact, we have previously shown that aerobic exercise improved functional capacity and attenuated systolic dysfunction during transition from compensated left ventricular hypertrophy to cardiac failure in rats with aortic stenosis [21-23].

Ascending aortic stenosis in rats has often been used to study chronic pressure overload. In this model, three-to-four week-old rats are subjected to thoracotomy to a clip placement around the ascending aorta. Immediately after clip positioning, aorta diameter is preserved; as rats get older, stenosis progressively occurs. Left ventricular hypertrophy development is fast occurring within one month [24]. However, ventricular dysfunction and cardiac failure develop slowly, similar to what is observed in human chronic pressure overload [24]. In this

study, we evaluated the influence of aerobic exercise performed during the transition from compensated left ventricular hypertrophy to overt heart failure on cardiac remodeling in rats with aortic stenosis. An important effect of exercise is the reduction in oxidative stress [25], which is associated with attenuation in cardiac remodeling. Therefore, we analyzed markers of systemic and myocardial oxidative stress, and activity of myocardial antioxidant enzymes. As the NADPH oxidase (NOX) family is a source of reactive oxygen species in various tissues including the myocardium [26], we analyzed gene expression of its subunits NOX2 and NOX4. Since mitogen-activated protein kinases (MAPK) may be involved in myocardial response to oxidative stress [27], we also evaluated their proteins expression in myocardium.

Materials and Methods

Experimental animals and study protocol

The experimental protocol employed in this study was approved by the Animal Experimentation Ethics Committee of Botucatu Medical School, UNESP, SP, Brazil, and has been previously described in detail [23]. Male Wistar rats (90 - 100 g) were purchased from the Central Animal House, Botucatu Medical School, UNESP, and housed in a temperature controlled room at 23 °C and kept on a 12-hour light/dark cycle. Food and water were supplied *ad libitum*.

In short, Wistar rats (90 - 100 g) were anaesthetized with a mixture of ketamine hydrochloride (50 mg/kg, i.m.) and xylazine hydrochloride (10 mg/kg, i.m.). Aortic stenosis (AS) was induced by placing a 0.6 mm stainless-steel clip on the ascending aorta via a thoracic incision [28]. Sham operated rats were used as controls. Eighteen weeks after surgery, rats were assigned to three groups: Sham (n=23), sedentary AS (AS, n=23), and exercised AS (AS-Ex, n=27) for eight weeks. During euthanasia, we assessed the presence or absence of clinical and pathologic heart failure features. The clinical finding suggestive of heart failure was tachypnea/labored respiration. Pathologic assessment of heart failure included pleuropericardial effusion, left atrial thrombi, ascites, hepatic congestion, pulmonary congestion (lung weight/body weight ratio higher than 2 standard deviations above the Sham group mean) and right ventricular hypertrophy (right ventricle weight/body weight ratio higher than 0.8 mg/g) [29]. Before and after the exercise protocol we evaluated functional capacity and performed transthoracic echocardiogram.

Exercise testing

Rats underwent 10 min/day testing environment adaption for one week before evaluations. Each animal was tested individually. The test consisted of an initial 5-min warm up at 5 m/min on treadmill. The rats were then subjected to exercise at a speed of 8 m/min followed by 3 m/min increases in speed every 3 min until exhaustion. Exhaustion was determined when the animal refused to run even

after electric stimulation or was unable to coordinate steps [30]. Maximum running speed was recorded and total distance calculated.

Exercise training protocol

Exercise was performed on a treadmill five times a week for eight weeks [23, 30, 31]. There was an adaptation period, with a gradual increase in speed and exercise time. Speed from the 1st to the 3rd week was 5, 7.5, and 10 m/min, and then remained constant until the end of the protocol. Exercise duration from the 1st to the 6th week was 10, 14, 18, 22, 26, and 30 min, and then remained constant until the end of the experiment.

Echocardiography

Cardiac structures and left ventricular function were evaluated by transthoracic echocardiogram and tissue Doppler imaging using a commercially available echocardiograph (General Electric Medical Systems, Vivid S6 model, Tirat Carmel, Israel) equipped with a 5-11.5 MHz multifrequency transducer [32-34]. The rats were anesthetized with a mixture of ketamine hydrochloride (50 mg/kg) and xylazine hydrochloride (1 mg/kg) intramuscularly. A two-dimensional parasternal short-axis view of the left ventricle (LV) was obtained at the level of the papillary muscles. M-mode tracings were obtained from short-axis views of the LV at or just below the tip of the mitral-valve leaflets, and at the level of the aortic valve and left atrium. M-mode images of the LV were printed on a black-and-white thermal printer (Sony UP-890MD) at a sweep speed of 100 mm/s. All LV structures were manually measured by the same observer (KO). Values obtained were the mean of at least five cardiac cycles on M-mode tracings. The following structural variables were measured: left atrium diameter (LA), LV diastolic and systolic diameters (LVDD and LVSD, respectively), LV diastolic (D) and systolic (S) posterior wall thickness (PWT) and septal wall thickness (SWT), and aortic diameter. LV mass (LVM) was calculated using the formula [(LVDD + DPWT + DSWT)3 - LVDD3] x 1.04. LV relative wall thickness (RWT) was calculated by the formula 2 x

DPWT/LVDD. LV function was assessed by the following parameters: endocardial fractional shortening (EFS), midwall fractional shortening (MFS), ejection fraction (EF), posterior wall shortening velocity (PWSV), early and late diastolic mitral inflow velocities (E and A waves), E/A ratio, E-wave deceleration time (EDT), and isovolumetric relaxation time (IVRT). A joint assessment of diastolic and systolic LV function was performed using the myocardial performance index (Tei index). The study was complemented with evaluation by tissue Doppler imaging (TDI) of systolic (S'), early diastolic (E'), and late diastolic (A') velocity of the mitral annulus (arithmetic average travel speeds of the lateral and septal walls), and E/E' ratio.

Collection of skeletal muscle and other tissues for analysis

One day after final echocardiogram, the rats were weighed, anesthetized with intraperitoneal sodium pentobarbital (50 mg/kg), and euthanized. After blood collecting, hearts were removed by thoracotomy. Atria and ventricles were dissected and weighed separately. LV was frozen in liquid nitrogen and stored at −80 °C. The liver was macroscopically examined to determine the presence or absence of liver congestion. Lung weight was used to assess the degree of pulmonary congestion [35].

Morphologic study

LV serial transverse 8 µm thick sections were cut in a cryostat cooled to -20 ºC and stained with hematoxylin and eosin. At least 50 cardiomyocyte diameters were measured from each LV as the shortest distance between borders drawn across the nucleus [30]. Other slides were stained with Sirius red F3BA and used to quantify interstitial collagen fraction [34]. On average, 20 microscopic fields were analyzed with a 40 X lens. Perivascular collagen was excluded from this analysis. Measurements were performed using a microscope (Leica DM LS; Nussloch, Germany) attached to a computerized imaging analysis system (Media Cybernetics, Silver Spring, MD, USA).

Oxidative stress evaluation

Myocardial glutathione concentration

Reduced glutathione was determined using a kinetic method in media consisting of 100 mM phosphate buffer pH 7.4 containing 5 mM EDTA, 2 mM 5.5'-dithiobis-(2-nitrobenzoic) acid (DTNB), 0.2 mM NADPH2 and 2 U of glutathione reductase [36]. Total glutathione was measured in the presence of 0.1 M Tris-HCl buffer, pH 8.0 with 0.5 mM EDTA, 0.6 mM DTNB and 0.1 U glutathione reductase [36].

Malondialdehyde serum concentration

Systemic lipid peroxidation was assessed by measuring malondialdehyde (MDA) by high performance liquid chromatography (HPLC), as previously reported [30]. Briefly, 100 μL of serum were treated with 700 μL of 1% orthophosphoric acid and vortex-mixed for 10 s for protein precipitation. Then, 200 μL of thiobarbituric acid (TBA) were added. The mixture was heated to 100 ºC for 60 min and cooled to -20 ºC for 10 min. Then, 200 μL of this reaction were added to a solution containing 200 μL of NaOH:methanol (1:12). The tubes were centrifuged for 3 min at 13,000 g; 200 μL of the supernatant were taken for injection in the equipment. Analysis was performed on a Shimadzu HPLC using a C18 5 μm Gemini Phenomenex column, and an Rf-535 fluorescence detector, which was set to Ex 525 nm and EM 551 nm. The mobile phase consisted of a 60:40 (v/v) mixture of 10 mmol potassium dihydrogen phosphate (pH 6.8):methanol. MDA was quantified by a calibration curve, which was constructed every day for analysis [37].

Antioxidant enzymes activity and lipid hydroperoxide concentration

Left ventricular samples (~200 mg) were homogenized in 5 mL of cold 0.1 M phosphate buffer, pH 7.0. Tissue homogenates were prepared in a motor-driven Teflon glass Potter-Elvehjem tissue homogenizer. The homogenate was

centrifuged at 10,000 g, for 15 min at 4 °C, and the supernatant was assayed for total protein, lipid hydroperoxide [38], and glutathione peroxidase (GSH-Px, E.C.1.11.1.9), catalase (E.C.1.11.1.6.), and superoxide dismutase (SOD, E.C.1.15.1.1.) activities by spectrophotometry [31]. Enzyme activities were analyzed at 25 °C using a microplate reader (μQuant-MQX 200) with KCjunior software for computer system control (Bio-Tech Instruments, Winooski, Vermont, USA). Spectrophotometric determinations were performed in a Pharmacia Biotech spectrophotometer with temperature controlled cuvette chamber (UV/visible Ultrospec 5000 with Swift II applications software for computer system control, Cambridge, UK). All reagents were purchased from Sigma-Aldrich (St. Louis, MO, USA).

Real-time quantitative reverse transcription-polymerase chain reaction (RT-PCR)

Gene expression of NADPH oxidase subunits (NOX2, NOX4, p22 phox, and p47 phox) and reference genes cyclophilin and glyceraldehyde-3-phosphate dehydrogenase (GAPDH) was analyzed by RT-PCR according to a previously described method [39]. Total RNA was extracted from LV myocardium with TRIzol Reagent (Invitrogen Life Technologies, Carlsbad, CA, USA) and treated with DNase I (Invitrogen Life Technologies). One microgram of RNA was reverse transcribed using High Capacity cDNA Reverse Transcription Kit, according to standard methods (Applied Biosystems, Foster City, CA, USA). Aliquots of cDNA were then submitted to real-time PCR reaction using a customized assay containing sense and antisense primers and Taqman (Applied Biosystems, Foster City, CA, USA) probes specific to each gene: NOX2 (Rn00576710 m1), NOX4 (Rn00585380 m1), p22 phox (Rn00577357 m1), and p47 phox (Rn00586945 m1). Amplification and analysis were performed using Step One Plus™ Real-Time PCR System (Applied Biosystems, Foster City, CA, USA). Expression data were normalized to reference gene expressions: cyclophilin (Rn00690933 m1) and GAPDH (Rn01775763 g1). Reactions were performed in triplicate and expression levels calculated using the CT comparative method ($2^{-\Delta\Delta CT}$).

Western blotting

Protein levels were analyzed by Western blotting using specific antibodies (Santa Cruz Biotechnology, Santa Cruz, CA, USA): total JNK1/2 (sc-137019), p-JNK (sc-6254), total p38-MAPK (sc-7972), p-p38-MAPK (sc-17852), total ERK 1 (sc-93), and p-ERK1/2 (sc-16982) [40, 41]. Protein levels were normalized to GAPDH (6C5 sc-32233). Myocardial protein was extracted using RIPA buffer (containing proteases and phosphatases inhibitors); supernatant protein content was quantified by the Bradford method. Samples were separated on a polyacrylamide gel and then transferred to a nitrocellulose membrane. After blockade, membrane was incubated with the primary antibodies. The membrane was then washed with TBS and Tween 20 and incubated with secondary peroxidase-conjugated antibodies. Super Signal ® West Pico Chemiluminescent Substrate (Pierce Protein Research Products, Rockford, USA) was used to detect bound antibodies.

Statistical analysis

Data are expressed as mean ± standard deviation or median and percentiles. Comparisons between groups were performed by one-way ANOVA and Tukey test or Kruskal-Wallis and Dunn test. Frequency of heart failure features was assessed by the Goodman test. Significance level was set at 5%.

Results

Heart failure features were evaluated at the euthanize. One Sham rat had ascites. The frequency of heart failure features in AS and AS-Ex groups is shown in Table 1. Except for a lower frequency of ascites in AS-Ex than AS, this frequency did not change between groups. Anatomical data are presented in Table 2. Both aortic stenosis groups had left and right ventricular hypertrophy, and atria and lung weights compared to the Sham. There were no differences between AS-Ex and AS groups.

Maximal exercise test is shown in Figure 1. Before exercise, running time was lower in both AS-and AS-Ex than Sham and running distance was lower in AS-Ex than Sham. After exercise protocol, running time and distance were lower in AS than Sham and were higher in AS-Ex than AS.

Echocardiographic evaluation before treatment is shown in Tables 3 and 4. AS and AS-Ex presented left atrium dilation and concentric LV hypertrophy, characterized by the increased LV walls thickness, LV mass, and relative wall thickness. LV diastolic diameter was higher in AS than Sham. Both AS-Ex and AS had LV systolic and diastolic dysfunction as posterior wall shortening velocity, isovolumetric relaxation time, and E wave deceleration time were lower and E wave and E/tissue Doppler imaging (TDI) of early diastolic velocity of mitral annulus were higher than Sham. TDI S' was in lower in AS than Sham. There were no differences between AS-Ex and AS.

Echocardiographic evaluation after exercise protocol showed the same cardiac remodeling pattern as before exercise. Additionally, both stenosis groups presented increased LV systolic and diastolic diameters, and E/A ratio, and decreased TDI S', and A wave. Endocardial and midwall fractional shortening and ejection fraction were lower in AS-Ex than Sham. No differences between AS-Ex and AS were observed (Tables 5 and 6).

Myocyte diameter and interstitial collagen fraction were higher in AS and AS-Ex than Sham. Myocyte diameter was higher in AS-Ex than AS (Table 7).

Total and reduced myocardial concentration of glutathione was lower in AS than Sham and total glutathione concentration was higher in AS-Ex than AS (Figure 2). Malondialdehyde serum concentration did not differ between groups. Lipid hydroperoxide myocardial concentration was higher in AS than Sham and AS-

Ex (Figure 3). Antioxidant enzyme activities in myocardium are shown in Figure 4. Superoxide dismutase was lower an both AS and AS-Ex than Sham and glutathione peroxidase was lower in AS-Ex than Sham.

Myocardial gene expression of NADPH oxidase subunits did not change between groups (Table 8). Myocardial expression of MAPK proteins is shown in Table 9. Phosphorylated JNK was higher in AS-Ex than Sham and AS groups and total JNK was higher in AS-Ex than Sham. Phosphorylated P38 was lower in AS-Ex than AS.

TABLES

Table 1. Frequency of heart failure features (%)

	AS (n=19)	AS-Ex (n=22)
Ascites	59.1	26.3#
Pleural effusion	27.3	52.6
Tachypnea	27.3	21.1
Atrial thrombi	36.4	47.4
Liver congestion	18.2	10.5
Lung congestion	59.1	68.4
Right ventricular hypertrophy	77.3	68.4

AS: aortic stenosis; AS-Ex: exercised aortic stenosis; n: number of animals. Goodman test; # p < 0.05 vs AS.

Table 2. Anatomical data

	Sham (n=23)	AS (n=19)	AS-Ex (n=22)
BW (g)	510 ± 50.7	482 ± 41.6	464 ± 57.5
LVW (g)	0.94 (0.88-0.98)	1.84 (1.56-2.09)*	1.48 (1.13-1.95)*
LVW/BW (mg/g)	1.86 (1.69-2.05)	3.80 (2.98-4.33)*	3.19 (2.23-5.05)*
RVW (g)	0.24 (0.21-0.25)	0.46 (0.40-0.55)*	0.43(0.36-0.46)*
RVW/BW (mg/g)	0.48 (0.45-0.50)	0.99 (0.83-1.11)*	0.89 (0.66-1.05)*
Atria weight (g)	0.10 (0.09-0.11)	0.36 (0.21-0.41)*	0.34 (0.31-0.41)*
Atria/BW (mg/g)	0.20 (0.19-0.23)	0.75 (0.66-0.82)*	0.71 (0.46-0.93)*
Lung weight (g)	1.80 (1.66-1.99)	2.89 (2.11-3.29)*	3.96 (2.31-4.37)*
Lung/BW (mg/g)	3.80 (3.12-4.11)	6.30 (4.29-7.05)*	8.41 (4.71-9.74)*

AS: aortic stenosis; AS-Ex: exercised aortic stenosis; BW: body weight; LVW: left ventricle weight; RVW: right ventricle weight. One-way ANOVA and Tukey or Kruskal-Wallis and Dunn test. Data are mean ± SD or median and percentiles; $*$ p < 0.05 versus Sham.

Table 3. Echocardiographic structural data before exercise protocol

	Sham (n=12)	AS (n=16)	AS-EX (n=15)
BW (g)	453 ± 62	442 ± 32	461 ± 57
LVDD (mm)	8.00 ± 0.55	8.87 ± 0.73*	8.52 ± 0.84
LVDD/BW (mm/kg)	17.4 (16.5 – 18.1)	20.1 (18.8 – 20.8)*	17.9 (16.6 – 19.3)
LVSD (mm)	3.75 ± 0.52	4.07 ± 0.93	4.03 ± 0.99
DPWT (mm)	1.43 (1.38 – 1.44)	2.07 (1.98 – 2.23)*	2.12 (1.53 – 2.25)*
SPWT (mm)	2.97 ± 0.28	3.92 ± 0.46*	3.63 ± 0.45*
DSWT (mm)	1.43 (1.40 – 1.44)	2.09 (1.98 – 2.23)*	2.12 (1.53 – 2.25)*
SSWT (mm)	2.49 (2.32 – 2.59)	3.11 (3.03 – 3.47)*	3.14 (2.72 – 3.47)*
RWT	0.36 (0.33 – 0.38)	0.48 (0.43 – 0.52)*	0.46 (0.38 – 0.53)*
AO (mm)	3.89 ± 0.28	3.84 ± 0.24	3.87 ± 0.23
LA (mm)	5.28 (4.93 – 5.66)	7.88 (6.21 – 8.54)*	7.66 (5.47 – 8.71)*
LA/AO	1.38 (1.33 – 1.42)	1.92 (1.62 – 2.34)*	2.05 (1.47 – 2.24)*
LA/BW (mm/kg)	11.6 (10.7 – 13.2)	18.1 (14.2 – 19.3)*	16.6 (12.1 – 19.9)*
LVM (g)	0.77 (0.73 – 0.86)	1.51 (1.32 – 1.80)*	1.60 (0.87 – 1.74)*
LVMI (g/kg)	1.72 (1.69 – 1.80)	3.45 (2.96 – 4.09)*	3.32 (1.85 – 3.68)*

AS: aortic stenosis; AS-Ex: exercised aortic stenosis; BW: body weight; LVDD and LVSD: left ventricular (LV) diastolic and systolic diameters, respectively; DPWT and SPWT: LV diastolic and systolic posterior wall thickness, respectively; DSWT and SSWT: LV diastolic and systolic septal wall thickness, respectively; RWT: relative wall thickness; AO: aorta diameter; LA: left atrial diameter; LVM: LV mass; LVMI: LVM index. One-way ANOVA and Tukey or Kruskal-Wallis and Dunn test. Data are mean ± SD or median and percentiles; $* p < 0.05$ vs Sham.

Table 4. Echocardiographic evaluation of left ventricular function before exercise protocol

	Sham (n=12)	AS (n=16)	AS-Ex (n=15)
HR (bpm)	259 ± 23	278 ± 43	283 ± 39
EFS (%)	53.3 ± 4.29	54.5 ± 7.79	53.2 ± 8.15
MFS (%)	31.4 ± 3.86	30.4 ± 5.92	29.7 ± 4.47
PWSV (mm/s)	38.8 (36.5 – 41.0)	29.6 (26.9 – 34.6)*	33.5 (30.4 – 38.4)*
Tei index	0.44 (0.39 – 0.49)	0.46 (0.39 – 0.51)	0.40 (0.37 – 0.53)
EF	0.90 ± 0.03	0.90 ± 0.05	0.89 ± 0.05
TDI S' (average, cm/s)	3.33 ± 0.38	2.83 ± 0.50*	2.98 ± 0.47
Mitral E (cm/s)	77 (71 – 81)	127 (96 – 144)*	113 (89 – 154)*
Mitral A (cm/s)	52 (46 – 57)	29 (19 – 59)	33 (18 – 77)
E/A	1.54 (1.34 – 1.62)	5.31 (1.63 – 6.71)	4.38 (1.26 – 7.89)
IVRT (ms)	26.0 ± 3.41	20.5 ± 5.90 *	19.3 ± 5.41*
IVRTn (ms)	53.1 (52.1 – 57.7)	40.8 (32.9 – 55.8)	40.7 (32.1 – 50.0)*
EDT (ms)	47.5 (43.0 – 75.0)	30.0 (26.0 – 45.8)*	29.5 (26.0 – 35.0)*
TDI E' (average, cm/s)	3.93 ± 0.62	3.77 ± 0.98	4.10 ± 0.67
TDI A' (average, cm/s)	3.15 (2.73 – 3.35)	3.23 (2.80 – 3.90)	3.15 (2.65 – 3.85)
E/TDI E' (average)	19.9 (16.9 – 22.6)	34.0 (27.9 – 39.7)*	30.1 (22.5 – 34.6)*

AS: aortic stenosis; AS-Ex: exercised aortic stenosis; HR: heart rate; EFS: endocardial fractional shortening; MFS: midwall fractional shortening; PWSV: posterior wall shortening velocity; Tei index: myocardial performance index; EF: ejection fraction; TDI S': tissue Doppler imaging (TDI) of systolic velocity of the mitral annulus; E/A: ratio between early (E)-to-late (A) diastolic mitral inflow; IVRT: isovolumetric relaxation time; IVRTn: IVRT normalized to heart rate; EDT: E wave deceleration time; TDI E' and A': TDI of early (E') and late (A') diastolic velocity of mitral annulus. One-way ANOVA and Tukey or Kruskal-Wallis and Dunn test. Data are mean ± SD or median and percentiles; * $p < 0.05$ vs Sham.

Table 5. Echocardiographic structural data after exercise protocol

	Sham (n=23)	AS (n=19)	AS-Ex (n=22)
BW (g)	504 ± 58	478 ± 50	461 ± 50*
LVDD (mm)	8.29 ± 0.54	9.16 ± 0.86*	9.11 ± 0.84*
LVDD/BW (mm/kg)	16.7 ± 2.04	19.3 ± 2.62*	20.0 ± 3.14*
LVSD (mm)	3.99 (3.58 – 4.50)	5.04 (4.06 – 5.34)*	5.12 (4.67 – 5.99) *
DPWT (mm)	1.42 (1.38 – 1.46)	2.05 (1.85 – 2.11)*	2.02 (1.84 – 2.17)*
SPWT (mm)	3.01 (2.75 – 3.14)	3.48 (2.87 – 3.79)*	3.49 (2.96 – 3.74)*
DSWT (mm)	1.43 (1.39 – 1.46)	2.11 (1.85 – 2.16)*	2.02 (1.84 – 2.17)*
SSWT (mm)	2.51 (2.38 – 2.64)	2.82 (2.65 – 3.16)*	3.00 (2.68 – 3.25)*
RWT	0.34 (0.33 – 0.36)	0.42 (0.40 – 0.47)*	0.44 (0.38 – 0.49)*
AO (mm)	4.02 (3.83 – 4.16)	3.94 (3.84 – 4.16)	3.97± 0.20
LA (mm)	5.29 (4.93 – 5.64)	8.54 (7.72 – 8.71)*	8.25 (7.15 – 8.98)*
LA/AO	1.34 (1.26 – 1.38)	2.17 (1.86 – 2.29)*	2.12 (1.75 – 2.25)*
LA/BW (mm/kg)	10.4 (9.53 – 12.1)	17.4 (14.8 – 19.5)*	17.6 (15.7 – 19.5)*
LVM (g)	0.82 (0.76 – 0.89)	1.41 (1.33 – 1.96)*	1.61 (1.18 – 1.87)*
LVMI (g/kg)	1.70 (1.46 – 1.87)	2.97 (2.70 – 3.90)*	3.40 (2.66 - 4.16)*

AS: aortic stenosis; AS-Ex: exercised aortic stenosis; BW: body weight; LVDD and LVSD: left ventricular (LV) diastolic and systolic diameters, respectively; DPWT and SPWT: LV diastolic and systolic posterior wall thickness, respectively; DSWT and SSWT: LV diastolic and systolic septal wall thickness, respectively; RWT: relative wall thickness; AO: aorta diameter; LA: left atrial diameter; LVM: LV mass; LVMI: LVM index. One-way ANOVA and Tukey or Kruskal-Wallis and Dunn test. Data are mean ± SD or median and percentiles; $*$ $p < 0.05$ vs Sham.

Table 6. Echocardiographic data of left ventricular function after exercise protocol

	Sham (n=23)	AS (n=19)	AS-Ex (n=22)
HR (bpm)	291 ± 40	295 ± 41	319 ± 41
EFS (%)	51.0 (46.4 – 55.3)	45.6 (38.7 – 55.3)	43.8 (38.3 – 48.2)*
MFS (%)	29.5 (27.2 – 32.4)	26.8 (21.1 – 33.5)	24.5 (21.6 – 28.6)*
PWSV (mm/s)	40.6 ± 5.55	30.8 ± 6.96*	29.2 ± 7.15*
Tei index	0.44 ± 0.08	0.42 ± 0.08	0.42 ± 0.11
EF	0.88 (0.85 – 0.91)	0.84 (0.77 – 0.91)	0.82 (0.77 – 0.86)*
TDI S' (average, cm/s)	3.76 ± 0.70	2.95 ± 0.67*	2.92 ± 0.49*
Mitral E (cm/s)	79.0 (72.3 – 83.5)	142 (85.0 – 158)*	142 (98 – 164)*
Mitral A (cm/s)	58.0 (51.5 - 67.0)	25.5 (22.0 – 47.0)*	20.0 (16.0 - 58.5)*
E/A	1.39 (1.23 – 1.52)	5.38 (1.74 – 6.82)*	8.00 (1.49 - 9.14)*
IVRT (ms)	26.0 (22.0 – 26.0)	18.0 (15.0 – 22.0)*	16.0 (15.0 - 22.0)*
IVRTn	53.0 ± 7.08	42.8 ± 11.0*	39.6 ± 10.3*
EDT (ms)	46.2 ± 6.87	31.1 ± 8.67*	30.1 ± 8.33*
TDI E' (average, cm/s)	4.51 ± 0.77	4.00 ± 1.26	4.23 ± 0.99
TDI A' (average, cm/s)	4.49 ± 1.34	3.91 ± 1.39	4.07 ± 1.05
E/TDI E' (average)	17.6 (14.7 – 19.8)	33.5 (26.5 - 41.0)*	34.3 (25.1 – 40.4)*

AS: aortic stenosis; AS-Ex: exercised aortic stenosis; HR: heart rate; EFS: endocardial fractional shortening; MFS: midwall fractional shortening; PWSV: posterior wall shortening velocity; Tei index: myocardial performance index; EF: ejection fraction; TDI S': tissue Doppler imaging (TDI) of systolic velocity of the mitral annulus; E/A: ratio between early (E)-to-late (A) diastolic mitral inflow; IVRT: isovolumetric relaxation time; IVRTn: IVRT normalized to heart rate; EDT: E wave deceleration time; TDI E' and A': TDI of early (E') and late (A') diastolic velocity of mitral annulus. One-way ANOVA and Tukey or Kruskal-Wallis and Dunn test. Data are mean ± SD or median and percentiles; * $p < 0.05$ vs Sham.

Table 7. Myocardial gene expression of NADPH oxidase subunits

	Sham (n=8)	AS (n=6)	AS-Ex (n=8)
p22 phox	1.00 ± 0.51	1.26 ± 0.98	1.33 ± 0.71
p47 phox	1.00 ± 0.48	0.89 ± 0.61	0.74 ± 0.43
NOX 2	0.74 (0.55-1.63)	1.64 (0.29-4.07)	1.12 (0.50-2.51)
NOX 4	1.01 (0.85-1.06)	3.47 (0.19-3.67)	1.39 (1.22-1.82)

AS: aortic stenosis; AS-Ex: exercised aortic stenosis. One-way ANOVA and Tukey test. Data are mean ± SD; $p > 0.05$.

Table 8. Myocardial morphometric parameters

	Sham (n=10)	AS (n=12)	AS-Ex (n=8)
Myocyte diameter (μm)	13.4 ± 1.17	15.1 ± 0.87*	16.7 ± 1.75*#
ICF (%)	4.30 ± 1.20	9.86 ± 1.69*	8.46 ± 1.61*

AS: aortic stenosis; AS-Ex: exercised aortic stenosis; ICF: interstitial collagen fraction. One-way ANOVA and Tukey test. Data are mean ± SD; * $p < 0.05$ vs Sham; # $p < 0.05$ vs AS.

Table 9. Myocardial expression of MAPK proteins

		Sham (n=7)	AS (n=7)	AS-Ex (n=7)
ERK	p-ERK/ERK	1.00 ± 0.22	1.46 ± 0.34*	1.33 ± 0.20
	p-ERK/GAPDH	1.00 ± 0.16	1.30 ± 0.85	1.74 ± 0.77
	ERK/GAPDH	1.00 ± 0.21	0.98 ± 0.41	1.23 ± 0.58
JNK	p-JNK/JNK	1.01 (0.86-1.07)	0.78 (0.68-1.27)	1.03 (0.94-1.72)
	p-JNK/GAPDH	1.07 (0.95-1.18)	1.15 (0.92-1.26)	1.88 (1.46-2.22)*#
	JNK/GAPDH	1.00 ± 0.23	1.11 ± 0.19	1.48 (1.29-1.73)*
P38	p-P38/P38	0.74 (0.50-1.68)	1.29 (1.23-1.81)	0.40 (0.26-0.70)
	p-P38/GAPDH	1.00 ± 0.54	2.01 ± 1.30	0.69 ± 0.41#
	P38/GAPDH	1.05 (0.81-1.13)	1.00 (0.70-2.58)	1.37 (0.92-1.92)

AS: aortic stenosis; AS-Ex: exercised aortic stenosis. One-way ANOVA and Tukey or Kruskal-Wallis and Dunn test. Data are mean ± SD or median and percentiles; * $p < 0.05$ vs Sham; # $p < 0.05$ vs AS.

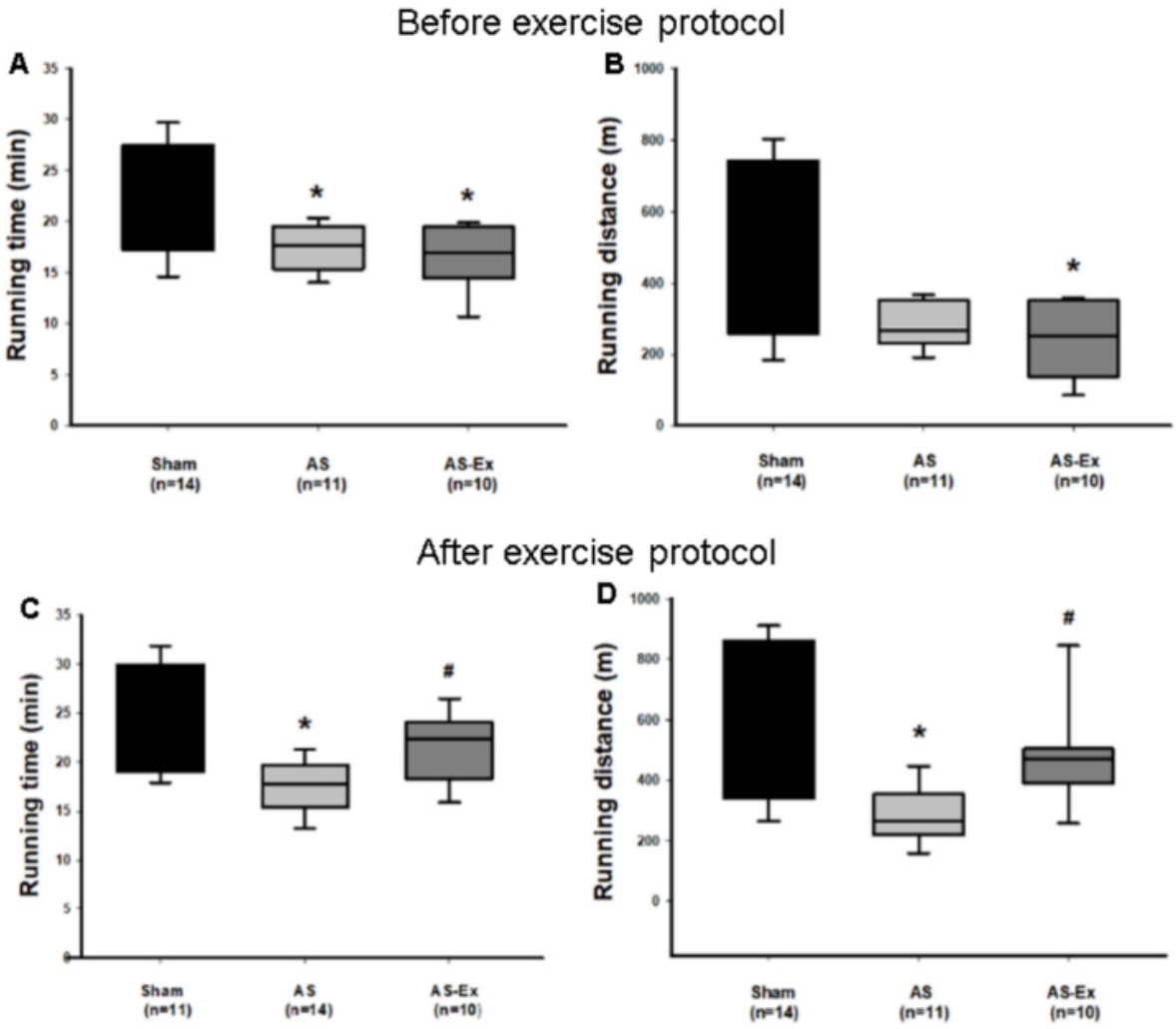

Figure 1. Maximal exercise test before and after physical training. Running time (A) and running distance (B) before exercise protocol; running time (C) and running distance (D) after exercise protocol. AS: aortic stenosis; AS-Ex: exercised aortic stenosis; n: number of animals. Data are median and percentiles; Kruskal-Wallis and Dunn test. * $p < 0.05$ vs Sham; # $p < 0.05$ vs AS.

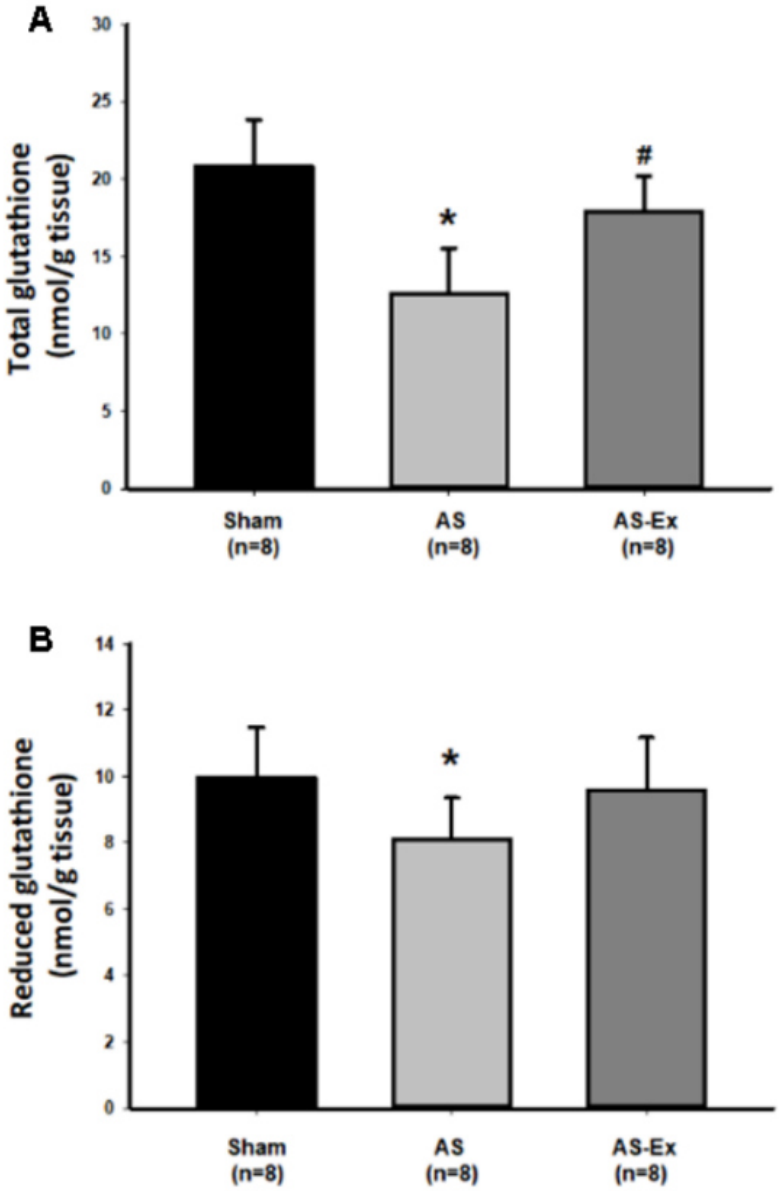

Figure 2. Myocardial concentration of total (A) and reduced glutathione (B). AS: aortic stenosis; AS-Ex: exercised aortic; n: number of animals. Data are mean ± SD; ANOVA and Tukey; * $p < 0.05$ vs Sham; # $p < 0.05$ vs AS.

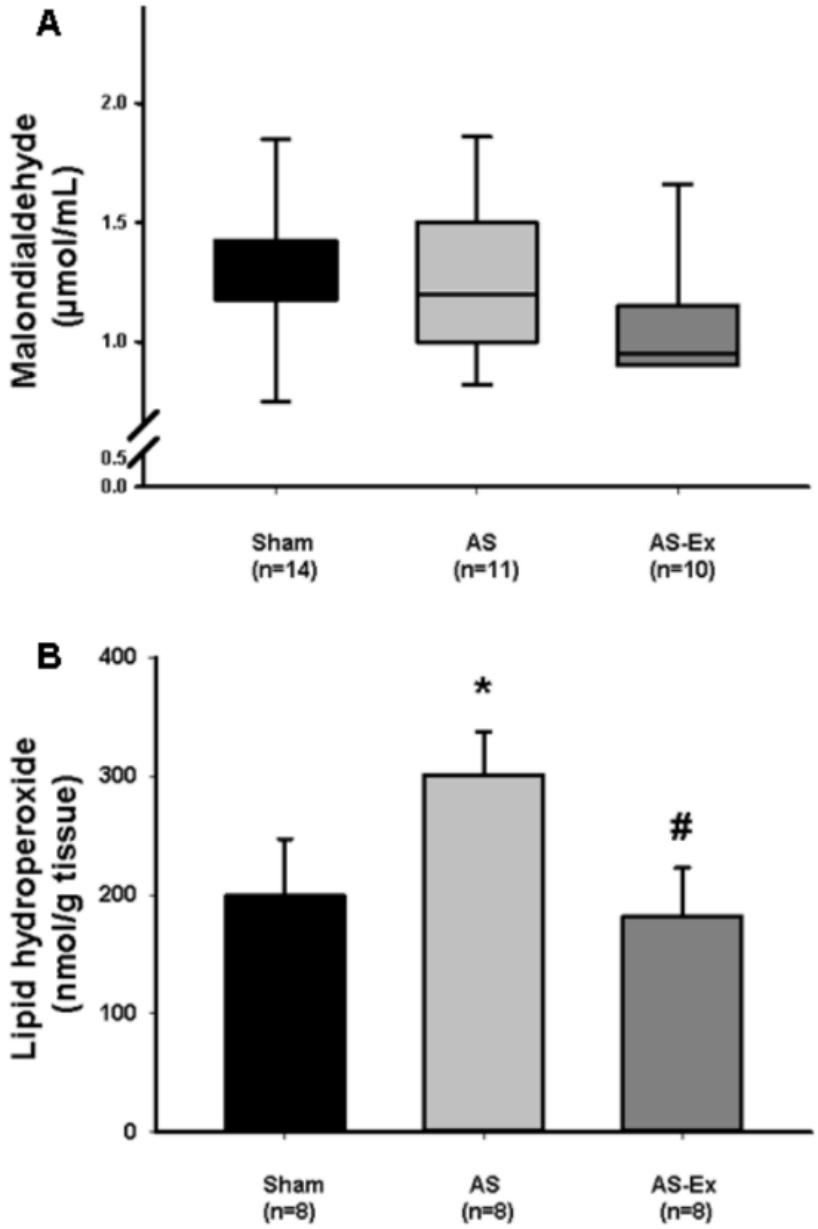

Figure 3. Malondialdehyde serum concentration (A) and lipid hydroperoxide myocardial concentration (B). AS: aortic stenosis; AS-Ex: exercised aortic stenosis; n: number of animals. Data are mean ± SD; ANOVA and Tukey or Kruskal-Wallis and Dunn test; * $p < 0.05$ vs Sham; # $p < 0.05$ vs AS.

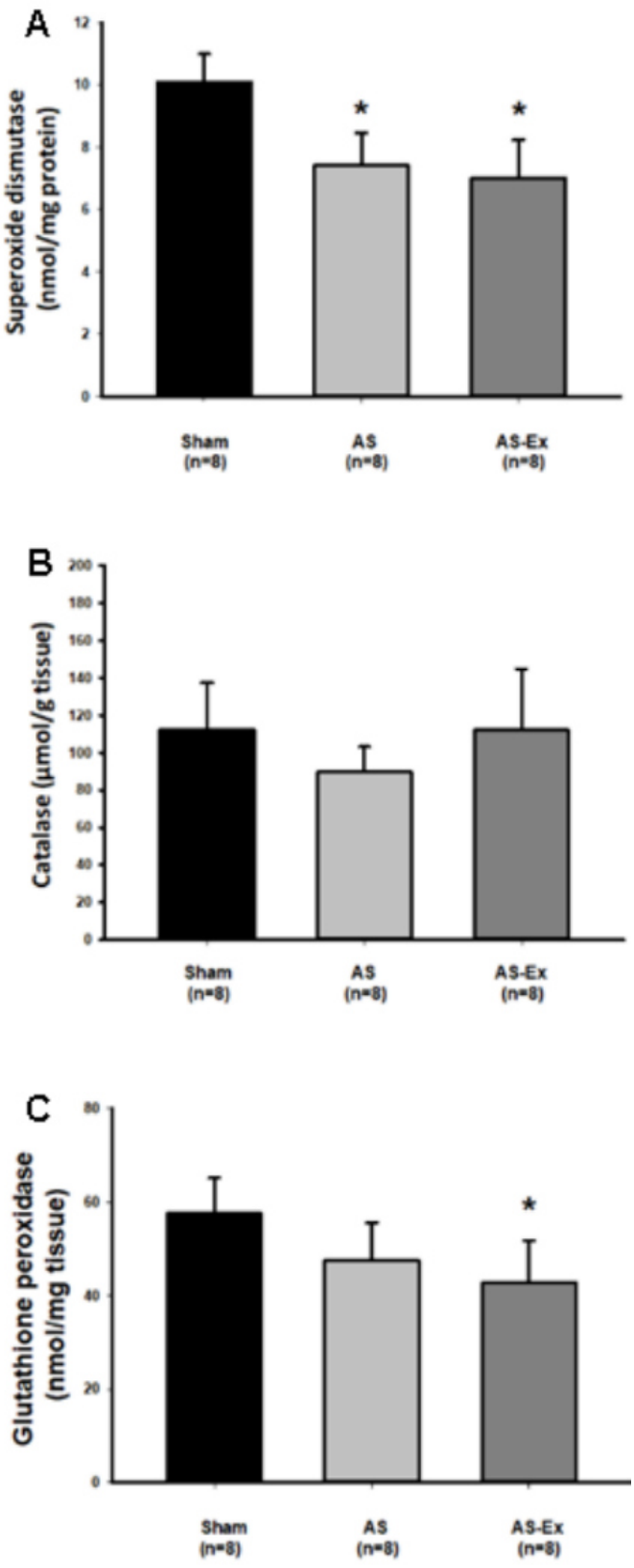

Figure 4. Antioxidant enzyme activities in myocardium. (A): superoxide dismutase; (B): catalase; (C): glutathione peroxidase. AS: aortic stenosis; AS-Ex: exercised aortic stenosis; n: number of animals. Data are mean ± SD; ANOVA and Tukey; * $p < 0.05$ vs Sham.

Discussion

In this study, we showed that aerobic exercise improves functional capacity in aortic stenosis rats during transition from left ventricular compensated hypertrophy to clinical heart failure. However, the improved physical capacity was not related to an improvement in cardiac structures or left ventricular function. We also performed the first evaluation of the influence of physical exercise on myocardial oxidative stress and MAPK signaling in aortic stenosis rats with heart failure.

Aortic stenosis rats have been often used to evaluate compensated left ventricular hypertrophy and its transition to clinical heart failure. After aortic stenosis induction, left ventricular hypertrophy can be observed within a month [24]. Rats then remain compensated for a period of 20 to 28 weeks, when they start to have clinical and pathological heart failure features and evolve to death in two to four weeks [21, 42]. In this study, the exercise protocol was initiated 18 weeks after aortic stenosis surgery; at this time, no rat had tachypnea/labored respiration.

Except for a lower frequency of ascites in AS-Ex than AS, exercise did not change the frequency of heart failure features. Before treatment, aortic stenosis rats presented left ventricular concentric hypertrophy with established diastolic dysfunction and mild systolic dysfunction. The same pattern of concentric hypertrophy was observed at the end of the experiment. Additionally, AS and AS-Ex had LV dilation and a more severe degree of diastolic dysfunction after the exercise protocol. There were no differences between AS-Ex and AS groups before and after the exercise protocol. However, in AS-Ex, the LV indexes of systolic function endocardial and midwall fractional shortening and ejection fraction were depressed when compared to the Sham group. Despite the impaired systolic function, functional capacity was better in AS-Ex than AS. Therefore, the better functional capacity in AS-Ex group was not related with an improvement in echocardiographic parameters. Studies on heart failure rats have suggested that exercise-induced improvement in skeletal muscle performance and metabolism is involved in the increased functional capacity [23, 43, 44].

Myocardial oxidative stress, evaluated by the lipid hydroperoxide concentration, was higher in AS than Sham and was normalized by exercise.

Exercise has long been shown to decrease oxidative stress in different experimental models [25, 31, 45].

Oxidative stress is characterized by an increase in the levels of reactive oxygen species and/or reactive nitrogen species. Both increased generation in reactive oxygen species and decreased antioxidant capacity can lead to oxidative stress [46]. Impaired antioxidant capacity can result from low concentrations of antioxidants and decreased antioxidant enzymes activity [46]. At physiological concentrations, reactive oxygen species play important roles in redox signaling and cell survival by modulating activity of different enzymes such as mitogen-activated protein kinase (MAPK), phosphatases, and gene-dependent cascades [46]. However, high levels of reactive oxygen species cause changes or injury to DNA, proteins, and lipids, and can stimulate apoptotic cell death [25, 47].

Myocytes consume high quantities of oxygen during muscle cell contraction and can generate a great amount of reactive oxygen species. Reactive oxygen species are mainly generated in mitochondria [46, 47]. They can also be produced in cytosol and membranes in response to different stimuli including growth factors and inflammatory cytokines [47]. Several enzymes including NADPH oxidase participate in ROS generation [48]. In this study, we showed for the first time that myocardial gene expression of the NADPH oxidase subunits NOX 2 and NOX 4 are not increased in aortic stenosis rats with heart failure and are not modulated by physical exercise.

Oxidative stress is neutralized by the antioxidant system, which includes endogenous and exogenous molecules. The main enzymatic defenses are superoxide dismutase, catalase, and glutathione peroxidase, which can be modified by exercise [25, 47]. In this study, superoxide dismutase was reduced in AS and AS-Ex compared to Sham and glutathione peroxidase was lower in AS-Ex than Sham. Catalase did not differ between groups. Exercise also preserved myocardial total and reduced glutathione.

Glutathione is an endogenous tripeptide that plays a central role in cellular defense against oxidative stress [49]. It is synthesized and maintained at high concentrations in most cells and is the main intracellular oxidant scavenger, protecting membranes, proteins, and DNA from oxidative stress [50]. In heart failure,

glutathione redox status is changed and its concentration is decreased in myocardium [51, 52]. Despite replenishment of total and reduced glutathione and normalization of lipid hydroperoxide, glutathione peroxidase activity remained lower in the AS-Ex group. Considering the levels of glutathione, it was surprising to observe a reduced glutathione peroxidase activity in AS-Ex compared to Sham. We have not identified studies evaluating physical exercise and myocardial oxidative stress in aortic stenosis rats. Therefore, additional studies are necessary to clarify the interplay between exercise and oxidative stress during transition from compensated left ventricular hypertrophy to clinical heart failure.

Exercise increased myocardial protein expression of total JNK and phosphorylated-JNK and reduced phosphorylated P38. The fact that JNK activation is related to myocyte hypertrophy may explain the greater myocyte diameter in AS-Ex than Sham and AS. Finally, myocardial fibrosis was evident in AS rats and was not modulated by physical exercise.

A large body of research spanning several decades has shown the safety and efficacy of regular physical activity in improving outcomes among heart failure patients, regardless of age, sex, or ethnicity [5-7, 15, 18, 53, 54]. Most clinical and experimental studies, however, have evaluated the remodeling of hearts with ischemic cardiomyopathy [55-58]. Nonetheless, the majority of experimental studies in genetic models of systemic hypertension [30, 59-61] as well as some clinical studies[62, 63], generally point towards a beneficial effect of regular exercise on cardiac hypertrophy and function. In fact, it was recently observed that the increase in functional capacity is independent of the heart failure aetiology [64]. Only a few studies have reported negative effects of long-term exercise in spontaneously hypertensive female rats [65] and aortic stenosis mice [19]. In these studies, however, both rats and mice exercised through voluntary rotating wheel, which is associated with excessive exercise. To the best of our knowledge, this is the first study to show that aerobic and controlled exercise is associated with an impaired cardiac remodeling in aortic stenosis rats.

One important component of exercise-induced improvement in left ventricular function is mediated via a reduction in peripheral impedance, which cannot be decreased in aortic constriction [19]. The results of this study show that

the beneficial effect of exercise in reducing oxidative stress and restore glutathione was preserved in the myocardium subjected to chronic and persistent pressure overload. However, in the presence of increased afterload and during transition from compensated hypertrophy to heart failure, the further overload caused by exercise resulted in additional myocyte hypertrophy, impaired signaling by the MAPK pathway, and a trend to impaired systolic function when compared to the sedentary AS rats. It is probable that the previously observed beneficial effects of exercise in chronic and persistent pressure overload [21, 22] occurred in early remodeling process and not during the transition to clinical heart failure, when rats present advanced degrees of left ventricular hypertrophy and dysfunction, thus preventing a reverse remodelling process.

In conclusion, aerobic exercise improves functional capacity in aortic stenosis rats during transition from left ventricular compensated hypertrophy to clinical heart failure independent of changes in cardiac structures or left ventricular function. Physical exercise reduces myocardial oxidative stress and glutathione peroxidase activity, and restores myocardial concentration of total and reduced glutathione. Despite the potential beneficial effects on oxidative stress, exercise induces further myocyte hypertrophy and impairs MAPK signaling.

References

1. Benjamin EJ, Blaha MJ, Chiuve SE, Cushman M, Das SR, Deo R, de Ferranti SD, Floyd J, Fornage M, Gillespie C, Isasi CR, Jimenez MC, Jordan LC, Judd SE, Lackland D, Lichtman JH, Lisabeth L, Liu S, Longenecker CT, Mackey RH, Matsushita K, Mozaffarian D, Mussolino ME, Nasir K, Neumar RW, Palaniappan L, Pandey DK, Thiagarajan RR, Reeves MJ, Ritchey M, Rodriguez CJ, Roth GA, Rosamond WD, Sasson C, Towfighi A, Tsao CW, Turner MB, Virani SS, Voeks JH, Willey JZ, Wilkins JT, Wu JH, Alger HM, Wong SS, Muntner P. American Heart Association Statistics Committee and Stroke Statistics Subcommittee. Heart disease and stroke statistics-2017 update: a report from the American Heart Association. *Circulation* 2017;135:e146-e603.

2. Drazner MH. The progression of hypertensive heart disease. *Circulation* 2011;123:327-334.

3. Ponikowski P, Voors AA, Anker SD, Bueno H, Cleland JG, Coats AJ, Falk V, González-Juanatey JR, Harjola VP, Jankowska EA, Jessup M, Linde C, Nihoyannopoulos P, Parissis JT, Pieske B, Riley JP, Rosano GM, Ruilope LM, Ruschitzka F, Rutten FH, van der Meer P. 2016 ESC Guidelines for the Diagnosis and Treatment of Acute and Chronic Heart Failure. The task force for the diagnosis and treatment of acute and chronic heart failure of the European Society of Cardiology (ESC) developed with the special contribution of the Heart Failure Association (HFA) of the ESC. *Eur Heart J* 2016;37:2129-2200.

4. Yancy CW, Jessup M, Bozkurt B, Butler J, Casey Jr. DE, Drazner MH, Fonarow GC, Geraci SA, Horwich T, Januzzi JL, Johnson MR, Kasper EK, Levy WC, Masoudi FA, McBride PE, McMurray JJ, Mitchell JE, Peterson PN, Riegel B, Sam F, Stevenson LW, Tang WH, Tsai EJ, Wilkoff BL. 2013 ACCF/AHA Guideline for the Management of Heart Failure: Executive summary. A report of the American College of Cardiology Foundation/American Heart Association task force on practice guidelines. *Circulation* 2013;128:1810-1852.

5. Ellingsen O, Halle M, Conraads V, Stoylen A, Dalen H, Delagardelle C, Larsen AI, Hole T, Mezzani A, Van Craenenbroeck EM, Videm V, Beckers P, Christle JW, Winzer E, Mangner N, Woitek F, Hollriegel R, Pressler A, Monk-Hansen T, Snoer

M, Feiereisen P, Valborgland T, Kjekshus J, Hambrecht R, Gielen S, Karlsen T, Prescott E, Linke A. Smartex Heart Failure Study (study of myocardial recovery after exercise training in heart failure) Group. High-intensity interval training in patients with heart failure with reduced ejection fraction. *Circulation* 2017;135:839-849.

6. Pandey A, Kitzman DW, Brubaker P, Haykowsky MJ, Morgan T, Becton JT, Berry JD. Response to endurance exercise training in older adults with heart failure with preserved or reduced ejection fraction. *J Am Geriatr Soc.*. 2017:in press.

7. Nakanishi M, Nakao K, Kumasaka L, Arakawa T, Fukui S, Ohara T, Yanase M, Noguchi T, Yasuda S, Goto Y. Improvement in exercise capacity by exercise training associated with favorable clinical outcomes in advanced heart failure with high B-type natriuretic peptide level. *Circ J* 2017:in press.

8. Garciarena CD, Pinilla OA, Nolly MB, Laguens RP, Escudero EM, Cingolani HE, Ennis IL. Endurance training in the spontaneously hypertensive rat. Conversion of pathological into physiological cardiac hypertrophy. *Hypertension* 2009;53:708-714.

9. Kraljevic J, Marinovic J, Pravdic D, Zubin P, Dujic Z, Wisloff U, Ljubkovic M. Aerobic interval training attenuates remodelling and mitochondrial dysfunction in the post-infarction failing rat heart. *Cardiovasc Res* 2013;99:55-64.

10. Llewellyn TL, Sharma NM, Zheng H, Patel KP. Effects of exercise training on sfo-mediated sympathoexcitation during chronic heart failure. *Am J Physiol Heart Circ Physiol* 2014;306:H121-H131.

11. Medeiros A, Rolim NP, Oliveira RS, Rosa KT, Mattos KC, Casarini DE, Irigoyen MC, Krieger EM, Krieger JE, Negrão CE, Brum PC. Exercise training delays cardiac dysfunction and prevents calcium handling abnormalities in sympathetic hyperactivity-induced heart failure mice. *J Appl Physiol* 2008;104:103-109.

12. Nunes RB, Alves JP, Kessler LP, Dal Lago P. Aerobic exercise improves the inflammatory profile correlated with cardiac remodeling and function in chronic heart failure rats. *Clinics* 2013;68:876-882.

13. Rossoni LV, Oliveira RA, Caffaro RR, Miana M, Sanz-Rosa D, Koike MK, Do Amaral SL, Michelini LC, Lahera V, Cachofeiro V. Cardiac benefits of exercise training in aging spontaneously hypertensive rats. *J Hypertens* 2011;29:2349-2358.

14. Xu X, Wan W, Powers AS, Li J, Ji LL, Lao S, Wilson B, Erikson JM, Zhang JQ. Effects of exercise training on cardiac function and myocardial remodeling in post myocardial infarction rats. *J Mol Cell Cardiol* 2008;44:114-122.

15. Slater RE, Strom JG, Granzier H. Effect of exercise on passive myocardial stiffness in mice with diastolic dysfunction. *J Mol Cell Cardiol* 2017;108:24-33.

16. Xu T, Zhang B, Yang F, Cai C, Wang G, Han Q, Zou L. Hsf1 and NF-κB p65 participate in the process of exercise preconditioning attenuating pressure overload-induced pathological cardiac hypertrophy. *Biochem Biophys Res Commun* 2015;460:622-627.

17. Grassi B, Majerczak J, Bardi E, Buso A, Comelli M, Chlopicki S, Guzik M, Mavelli I, Nieckarz Z, Salvadego D, Tyrankiewicz U, Skorka T, Bottinelli R, Zoladz JA, Pellegrino MA. Exercise training in tgαq*44 mice during the progression of chronic heart failure: cardiac vs. peripheral (soleus muscle) impairments to oxidative metabolism. *J Appl Physiol* 2017:in press.

18. Adams V, Reich B, Uhlemann M, Niebauer J. Molecular effects of exercise training in patients with cardiovascular disease: focus on skeletal muscle, endothelium, and myocardium. *Am J Physiol Heart Circ Physiol* 2017;313:H72-H88.

19. van Deel ED, Boer M, Kuster DW, Boontje NM, Holemans P, Sipido KR, van der Velden J, Duncker DJ. Exercise training does not improve cardiac function in compensated or decompensated left ventricular hypertrophy induced by aortic stenosis. *J Mol Cell Cardiol* 2011;50:1017-1025.

20. Lerman I, Harrison BC, Freeman K, Hewett TE, Allen DL, Robbins J, Leinwand LA. Genetic variability in forced and voluntary endurance exercise performance in seven inbred mouse strains. *J Appl Physiol* 2002;92:2245-2255.

21. Souza RW, Piedade WP, Soares LC, Souza PA, Aguiar AF, Vechetti-Júnior IJ, Campos DH, Fernandes AA, Okoshi K, Carvalho RF, Cicogna AC, Dal-Pai-Silva M. Aerobic exercise training prevents heart failure-induced skeletal muscle atrophy by anti-catabolic, but not anabolic actions. *PLoS One* 2014;9:e110020.

22. Souza RW, Fernandez GJ, Cunha JP, Piedade WP, Soares LC, Souza PA, de Campos DH, Okoshi K, Cicogna AC, Dal-Pai-Silva M, Carvalho RF. Regulation of cardiac microRNAs induced by aerobic exercise training during heart failure. *Am J Physiol Heart Circ Physiol* 2015;309:H1629-H1641.

23. Gomes MJ, Martinez PF, Campos DHS, Pagan LU, Bonomo C, Lima AR, Damatto RL, Cezar MD, Damatto FC, Rosa CM, Garcia CM, Reyes DA, Fernandes AA, Fernandes DC, Laurindo FR, Okoshi K, Okoshi MP. Beneficial effects of physical exercise on functional capacity and skeletal muscle oxidative stress in rats with aortic stenosis-induced heart failure. *Oxid Med Cell Longev* 2016;2016:8695716.

24. Ribeiro HB, Okoshi K, Cicogna AC, Bregagnollo EA, Rodrigues MAM, Padovani CR, Aragon FF, Jamas E, Okoshi MP. Estudo evolutivo da morfologia e função cardíaca em ratos submetidos a estenose aórtica supravalvar. *Arq Bras Cardiol* 2003;81:562-568.

25. Gomes MJ, Martinez PF, Pagan LU, Damatto RL, Cezar MD, Lima AR, Okoshi K, Okoshi MP. Skeletal muscle aging: influence of oxidative stress and physical exercise. *Oncotarget* 2017;8:20428-20440.

26. Bedard K, Krause KH. The NOX family of ROS-generating NADPH oxidases: physiology and pathophysiology. *Physiol Rev* 2007;87:245-313.

27. Martinez PF, Bonomo C, Guizoni DM, Junior SA, Damatto RL, Cezar MD, Lima AR, Pagan LU, Seiva FR, Bueno RT, Fernandes DC, Laurindo FR, Zornoff LA, Okoshi K, Okoshi MP. Modulation of MAPK and NF-kappaB signaling pathways

by antioxidant therapy in skeletal muscle of heart failure rats. *Cell Physiol Biochem* 2016;39:371-384.

28. Moreira VO, Pereira CA, Silva MO, Felisbino SL, Cicogna AC, Okoshi K, Aragon FF, Padovani CR, Okoshi MP, Castro AV. Growth hormone attenuates myocardial fibrosis in rats with chronic pressure overload-induced left ventricular hypertrophy. *Clin Exp Pharmacol Physiol* 2009;36:325-330.

29. Martinez PF, Okoshi K, Zornoff LA, Oliveira SAJ, Campos DH, Lima AR, Damatto RL, Cezar MD, Bonomo C, Guizoni DM, Padovani CR, Cicogna AC, Okoshi MP. Echocardiographic detection of congestive heart failure in postinfarction rats. *J Appl Physiol* 2011;111:543-551.

30. Pagan LU, Damatto RL, Cezar MD, Lima AR, Bonomo C, Campos DH, Gomes MJ, Martinez PF, Oliveira SAJ, Gimenes R, Rosa CM, Guizoni DM, Moukbel YC, Cicogna AC, Okoshi MP, Okoshi K. Long-term low intensity physical exercise attenuates heart failure development in aging spontaneously hypertensive rats. *Cell Physiol Biochem* 2015;36:61-74.

31. Gimenes C, Gimenes R, Rosa CM, Xavier NP, Campos DHS, Fernandes AAH, Cezar MDM, Guirado GN, Cicogna AC, Takamoto AHR, Okoshi MP, Okoshi K. Low intensity physical exercise attenuates cardiac remodeling and myocardial oxidative stress and dysfunction in diabetic rats. *J Diabetes Res* 2015:ID 457848.

32. Cezar MD, Damatto RL, Pagan LU, Lima AR, Martinez PF, Bonomo C, Rosa CM, Campos DH, Cicogna AC, Gomes MJ, Oliveira-Jr SA, Blotta DA, Okoshi MP, Okoshi K. Early spironolactone treatment attenuates heart failure development by improving myocardial function and reducing fibrosis in spontaneously hypertensive rats. *Cell Physiol Biochem* 2015;36:1453-1466.

33. Damatto RL, Martinez PF, Lima AR, Cezar MD, Campos DH, Oliveira SAJ, Guizoni DM, Bonomo C, Nakatani BT, Dal Pai Silva M, Carvalho RF, Okoshi K, Okoshi MP. Heart failure-induced skeletal myopathy in spontaneously hypertensive rats. *Int J Cardiol* 2013;167:698-703.

34. Okoshi MP, Cezar MD, Iyomasa RM, Silva MB, Costa LC, Martinez PF, Campos DH, Damatto RL, Minicucci MF, Cicogna AC, Okoshi K. Effects of early aldosterone antagonism on cardiac remodeling in rats with aortic stenosis-induced pressure overload. *Int J Cardiol* 2016;222:569-575.

35. Damatto RL, Lima AR, Martinez PF, Cezar MD, Okoshi K, Okoshi MP. Myocardial myostatin in spontaneously hypertensive rats with heart failure. *Int J Cardiol* 2016;215:384-387.

36. Tietze F. Enzymic method for quantitative determination of nanogram amounts of total and oxidized glutathione: applications to mammalian blood and other tissues. *Anal Biochem* 1969;27:502-522.

37. Nielsen F, Mikkelsen BB, Nielsen JB, Andersen HR, Grandjean P. Plasma malondialdehyde as biomarker for oxidative stress: reference interval and effects of life-style factors. *Clin Chem* 1997;43:1209-1214.

38. Rosa CM, Gimenes R, Campos DH, Guirado GN, Gimenes C, Fernandes AA, Cicogna AC, Queiroz RM, Falcão-Pires I, Miranda-Silva D, Rodrigues P, Laurindo FR, Fernandes DC, Correa CR, Okoshi MP, Okoshi K. Apocynin influence on oxidative stress and cardiac remodeling of spontaneously hypertensive rats with diabetes mellitus. *Cardiovasc Diabetol* 2016;15:126.

39. Martinez PF, Bonomo C, Guizoni DM, Junior SA, Damatto RL, Cezar MD, Lima AR, Pagan LU, Seiva FR, Fernandes DC, Laurindo FRM, Novelli EL, Matsubara LS, Zornoff LA, Okoshi K, Okoshi MP. Influence of N-acetylcysteine on oxidative stress in slow-twitch soleus muscle of heart failure rats. *Cell Physiol Biochem* 2015;35:148-159.

40. Lima AR, Martinez PF, Okoshi K, Guizoni DM, Zornoff LA, Campos DH, Oliveira SAJ, Bonomo C, Pai-Silva MD, Okoshi MP. Myostatin and follistatin expression in skeletal muscles of rats with chronic heart failure. *Int J Exp Path* 2010;91:54-62.

41. Lima AR, Martinez PF, Damatto RL, Cezar MD, Guizoni DM, Bonomo C, Oliveira SAJ, Dal-Pai Silva M, Zornoff LA, Okoshi K, Okoshi MP. Heart failure-induced diaphragm myopathy. *Cell Physiol Biochem* 2014;34:333-345.

42. Boluyt MO, Robinson KG, Meredith AL, Sen S, Lakatta EG, Crow MT, Brooks WW, Conrad CH, Bing OHL. Heart failure after long-term supravalvar aortic constriction in rats. *Am J Hypertens* 2005;18:202-212.

43. Okoshi MP, Romeiro FG, Paiva SA, Okoshi K. Heart failure-induced cachexia. *Arq Bras Cardiol* 2013;100:476-482.

44. Okoshi MP, Capalbo RV, Romeiro FG, Okoshi K. Cardiac cachexia: perspectives for prevention and treatment. *Arq Bras Cardiol* 2017;108:74-80.

45. Lu K, Wang L, Wang C, Yang Y, Hu D, Ding R. Effects of high-intensity interval versus continuous moderate-intensity aerobic exercise on apoptosis, oxidative stress and metabolism of the infarcted myocardium in a rat model. *Mol Med Rep* 2015;12:2374-2382.

46. Altenhofer S, Radermacher KA, Kleikers PW, Wingler K, Schmidt HH. Evolution of nadph oxidase inhibitors: selectivity and mechanisms for target engagement. *Antioxid Redox Signal* 2015;23:406-427.

47. Bouzid MA, Filaire E, McCall A, Fabre C. Radical oxygen species, exercise and aging: an update. *Sports Med* 2015;45:1245-1261.

48. Ferreira LF, Laitano O. Regulation of NADPH oxidases in skeletal muscle. *Free Radic Biol Med* 2016;98:18-28.

49. Fratelli M, Goodwin LO, Orom UA, Lombardi S, Tonelli R, Mengozzi M, Ghezzi P. Gene expression profiling reveals a signaling role of glutathione in redox regulation. *Proc Natl Acad Sci U S A* 2005;102:13998-14003.

50. Rushworth GF, Megson IL. Existing and potential therapeutic uses for N-acetylcysteine: the need for conversion to intracellular glutathione for antioxidant benefits. *Pharmacol Ther* 2014;141:150-159.

51. Adamy C, Mulder P, Khouzami L, Andrieu-Abadie N, Defer N, Candiani G, Pavoine C, Caramelle P, Souktani R, Le Corvoisier P, Perier M, Kirsch M, Damy T, Berdeaux A, Levade T, Thuillez C, Hittinger L, Pecker F. Neutral sphingomyelinase inhibition participates to the benefits of N-acetylcysteine treatment in post-myocardial infarction failing heart rats. *J Mol Cell Cardiol* 2007;43:344-353.

52. Lombardi R, Rodriguez G, Chen SN, Ripplinger CM, Li W, Chen J, Willerson JT, Betocchi S, Wickline SA, Efimov IR, Marian AJ. Resolution of established cardiac hypertrophy and fibrosis and prevention of systolic dysfunction in a transgenic rabbit model of human cardiomyopathy through thiol-sensitive mechanisms. *Circulation* 2009;119:1398-1407.

53. Coats AJS, Forman DE, Haykowsky M, Kitzman DW, McNeil A, Campbell TS, Arena R. Physical function and exercise training in older patients with heart failure. *Nat Rev Cardiol* 2017:in press.

54. Pearson MJ, Mungovan SF, Smart NA. Effect of exercise on diastolic function in heart failure patients: a systematic review and meta-analysis. *Heart Fail Rev* 2017;22:229-242.

55. de Waard MC, van der Velden J, Bito V, Ozdemir S, Biesmans L, Boontje NM, Dekkers DH, Schoonderwoerd K, Schuurbiers HC, de Crom R, Stienen GJ, Sipido KR, Lamers JM, Duncker DJ. Early exercise training normalizes myofilament function and attenuates left ventricular pump dysfunction in mice with a large myocardial infarction. *Circ Res* 2007;100:1079-1088.

56. Crimi E, Ignarro LJ, Cacciatore F, Napoli C. Mechanisms by which exercise training benefits patients with heart failure. *Nat Rev Cardiol* 2009;6:292-300.

57. Haykowsky MJ, Liang Y, Pechter D, Jones LW, McAlister FA, Clark AM. A meta-analysis of the effect of exercise training on left ventricular remodeling in heart failure patients: the benefit depends on the type of training performed. *J Am Coll Cardiol* 2007;49:2329-2336.

58. Campos JC, Queliconi BB, Bozi LHM, Bechara LRG, Dourado PMM, Andres AM, Jannig PR, Gomes KMS, Zambelli VO, Rocha-Resende C, Guatimosim S, Brum PC, Mochly-Rosen D, Gottlieb RA, Kowaltowski AJ, Ferreira JCB. Exercise reestablishes autophagic flux and mitochondrial quality control in heart failure. *Autophagy* 2017:in press.

59. Chicco AJ, McCune SA, Emter CA, Sparagna GC, Rees ML, Bolden DA, Marshall KD, Murphy RC, Moore RL. Low-intensity exercise training delays heart failure and improves survival in female hypertensive heart failure rats. *Hypertension* 2008;51:1096-1102.

60. MacDonnell SM, Kubo H, Crabbe DL, Renna BF, Reger PO, Mohara J, Smithwick LA, Koch WJ, Houser SR, Libonati JR. Improved myocardial beta-adrenergic responsiveness and signaling with exercise training in hypertension. *Circulation* 2005;111:3420-3428.

61. Miyachi M, Yazawa H, Furukawa M, Tsuboi K, Ohtake M, Nishizawa T, Hashimoto K, Yokoi T, Kojima T, Murate T, Yokota M, Murohara T, Koike Y, Nagata K. Exercise training alters left ventricular geometry and attenuates heart failure in dahl salt-sensitive hypertensive rats. *Hypertension* 2009;53:701-707.

62. Boman K, Gerdts E, Wachtell K, Dahlof B, Nieminen MS, Olofsson M, Papademetriou V, Devereux RB. Exercise and cardiovascular outcomes in hypertensive patients in relation to structure and function of left ventricular hypertrophy: The LIFE Study. *Eur J Cardiovasc Prev Rehabil* 2009;16:242-248.

63. Palatini P, Visentin P, Dorigatti F, Guarnieri C, Santonastaso M, Cozzio S, Pegoraro F, Bortolazzi A, Vriz O, Mos L. Harvest study group. Regular physical activity prevents development of left ventricular hypertrophy in hypertension. *Eur Heart J* 2009;30:225-232.

64. Antunes-Correa LM, Ueno-Pardi LM, Trevizan PF, Santos MR, da Silva CH, Franco FG, Alves MJ, Rondon MU, Negrao CE. The influence of aetiology on the benefits of exercise training in patients with heart failure. *Eur J Prev Cardiol* 2017;24:365-372.

65. Schultz RL, Swllow JG, Waters RP, Kuzman JA, Redetzke RA, Said S, Escobar GM, Gerdes AM. Effects of excessive long-term exercise on cardiac function and myocyte remodeling in hypertensive heart failure rats. *Hypertension* 2007;50:410-416.